CANADIAN THESES

THÈSES CANADIENNES

NOTICE

The quality of this microfiche is heavily dependent upon the quality of the original thesis submitted for microfilming. Every effort has been made to ensure the highest quality of reproduction possible.

If pages are missing, contact the university which granted the degree.

Some pages may have indistinct print especially if the original pages were typed with a poor typewriter ribbon or if the university sent us an inferior photocopy.

Previously copyrighted materials (journal articles, published tests, etc.) are not filmed.

Reproduction in full or in part of this film is governed by the Canadian Copyright Act, R.S.C. 1970, c. C-30.

AVIS

La qualité de cette microfiche dépend grandement de la qualité de la thèse soumise au microfilmage. Nous avons tout fait pour assurer une qualité supérieure de reproduction.

S'il manque des pages, veuillez communiquer avec l'université qui a conféré le grade.

La qualité d'impression de certaines pages peut laisser à désirer, surtout si les pages originales ont été dactylographiées à l'aide d'un ruban usé ou si l'université nous a fait parvenir une photocopie de qualité inférieure.

Les documents qui font déjà l'objet d'un droit d'auteur (articles de revue, examens publiés, etc.) ne sont pas microfilmés.

La reproduction, même partielle, de ce microfilm est soumise à la Loi canadienne sur le droit d'auteur, SRC 1970, c. C-30.

THIS DISSERTATION HAS BEEN MICROFILMED EXACTLY AS RECEIVED

LA THÈSE A ÉTÉ MICROFILMÉE TELLE QUE NOUS L'AVONS REÇUE

Comparative Study on Sandwich Plate Finite Elements

Behdad Jafari-Naini

A Thesis

in

The Center

for

Building Studies

Presented in Partial Fulfillment of the Requirements
for the Degree of Master of Engineering at
Concordia University
Montreal, Quebec, Canada

December 1985

ISBN 0-315-30610-6

ABSTRACT

Comparative Study on Sandwich Plate Finite Elements

Behdad Jafari-Naini

The theories dealing with sandwich plates diverge from classical thin plate theory in that they include the effects of transverse shear strains in the core. The use of sandwich plates in the construction industry has been partially hindered by the lack of general analytical solutions. The finite element method has proved to be a powerful analysis tool in these situations.

In this study, several finite elements suitable for analysis of three layer flat sandwich plates subjected to transverse loading have been considered. These elements have been divided into two groups of displacement and assumed stress hybrid elements based on the method used in the derivation of their stiffness matrix. These two methods have been briefly outlined and compared.

The characteristics and the range of applicability of elements in each group have been discussed. Several numerical tests were carried out in order to evaluate the performance of assumed stress hybrid elements. Finally, an experimental element has been introduced and its performance has been studied.

ACKNOWLEDGEMENTS

I would like to express my gratitude to Dr. H. K. Ha for his invaluable guidance throughout this study.

I am sincerely thankful to Dr. Anthony Firmin for his full support and his helpful comments in the course of preparation of this report.

Thanks are due to Allan, Gowri, Luong, Martin and Parvaneh who, with their presence and help, made the graduate work at CBS a more enjoyable experience.

Finally, I am thankful to my family for their patience and understanding.

TABLE OF CONTENTS

LIST OF FIGURES

LIST OF TABLES

NOTATIONS

a	dimension of plate parallel to X-axis
AR	aspect ratio of a plate
b	dimension of plate parallel to Y-axis
B, B_x, B_y	bending stiffness of a section
c	core thickness
d	distance between centroids of two adjacent faces
D, D_x, D_y	flexural stiffness of a section
E_f, E_c	Young modulus for face and core materials
G	shear modulus for core material
m	number of independent stress parameters
M_{xx}, M_{yy}	normal moments per unit length
M_{xy}, M_{yx}	twisting moments per unit length
n	number of element degrees of freedom
q	transverse load on a plate
Q_x, Q_y	transverse shear forces per unit length
r	number of rigid body modes in an element
s	length along the boundary of an element
S, S_x, S_y	shear stiffness of a section
$\underline{S}$	surface of an element
SP	shear parameter
t	face thickness
T	twisting stiffness of a section
U	strain energy of an element
U_0	strain energy density in an element
V	potential energy of applied loads
$\underline{V}$	volume of an element
u, u_x, u_y, u_{xy}	displacement in x direction and its derivatives
v, v_x, v_y, v_{xy}	displacement in y direction and its derivatives
w, w_x, w_y, w_z	displacement in z direction and its derivatives
w_{xx}, w_{yy}, w_{xy}	curvatures
$[B]$	matrix relating strains to displacements
$[C]$	matrix relating strains to stresses
$\{d\}$	nodal degrees of freedom
$[E]$	matrix relating stresses to strains

$[H]$	matrix used for hybrid elements
$[K]$	element stiffness matrix
$[L]$	boundary shape functions for hybrid elements
$[N]$	shape functions for displacement elements
$\{p\}$	applied load vector
$[P]$	stress distribution matrix for hybrid elements
$\{Q\}$	element load vector
$[R]$, $[S]$, $[T]$	matrices used for hybrid elements
$\{u\}$	displacement field vector
γ, γ_x, γ_y	transverse shear strains
υ_x, υ_y	poisson ratios
Π	total potential energy of an element
Π_c	total complementary energy of an element
θ_x, θ_y	rotations of normals about x and y axes
ξ	normalized coordinate along the edges
$\{\beta\}$	vector of independent stress parameters
$\{\epsilon\}$	strain vector
$\{\sigma\}$	stress vector

CHAPTER I

INTRODUCTION

1.1 Description of Sandwich Construction

Sandwich construction is a special type of multilayer construction where thin sheets of high stiffness materials are bonded to relatively thick layers of lower stiffness and density. In the case of three layer construction, the outer sheets are called faces and the inner thick layer is referred to as a core. The idea behind this type of construction is to place the high stiffness materials as far as possible from the neutral axis, where they are more efficient in resisting bending stresses, without excessively increasing the weight of the section. As a result, this type of construction usually has a higher strength to weight ratio than the conventional types of construction.

In a sandwich section, the faces are the main stress carrying components due to their position and high stiffness and resist primarily fiber stresses parallel to the neutral axis. Typical materials for the faces

include steel, aluminum alloys, reinforced plastics and titanium.

The function of the core is to provide shear resistance and lateral stability for the section and thus should be strong enough to resist transverse normal as well as shear stresses. Because of the low stiffness of the core material, the in-plane stresses in the core are small and the contribution of the core to the flexural rigidity of the section is often neglected. The core usually deforms under transverse shear stresses and therefore, it is no longer possible to assume that normals to the mid-planes remain normal after deformation. The core is made of lighter and weaker materials such as synthetic rubber or styrofoam which could enable the core to act as thermal insulator for the structure. Honeycomb and corrugated cores have also been successively used in sandwich construction.

The bond between the adjacent layers is very important and is usually achieved by means of various types of adhesives. The bond must be strong enough to maintain continuity of displacements across different layers. In the absence of strong bonds, interlayer slip may occur and as a result, the structural efficiency of sandwich construction may suffer.

Finally, it is important to distinguish between sandwich construction and composite laminates. The latter consists of various layers of similar properties which contribute to resisting stresses in a similar way. Shear deformation is generally not dominant in any layer and it is often assumed that the normals to the mid-plane remain normals after the deformation. However, it is possible that some layers of a composite laminate undergo significant transverse shear deformation. In such cases, sandwich construction could be thought of as a special case of composite laminates where only alternate layers deform under transverse shear.

1.2 Objectives and Organization of the Thesis

The theories dealing with the analysis of sandwich plates have been developed since the late forties. These theories diverge from the classical thin plate theory in that they take into account the transverse shear deformations in the core. However, as in the case of thin plate theory, analytical solutions are often cumbersome and limited to cases with relatively simple boundary and loading conditions. The development of the finite element method has paved the way for the solution of more complex

problems. Since the late sixties, a number of finite elements have been developed for application to sandwich plate analysis. These elements which cover a wide range of capabilities, can be classified into two groups based on the method used in deriving their stiffness matrices. In the first group are the displacement elements which are based on the minimization of the total potential energy and in the second group are the assumed stress hybrid elements which are based on the minimization of the total complementary energy.

Although the existence of these elements has facilitated the analysis of sandwich plates, choosing a suitable element remains a difficult task. As often is the case, the underlying assumptions for the elements may differ and consequently the range of applicability of the elements are not clear. Unfortunately, at times neither the assumptions nor the extent of the capabilities of an element have been explicitly stated. Some of these characteristics may have been demonstrated by the authors through the various numerical tests they have performed. However, the test problems may differ from one element to the next, thus making the comparison of the results between two or more elements difficult if not impossible.

The objective of this study is to facilitate the task of choosing a suitable element by:

1 - examining the underlying assumptions,

2 - determining the range of capabilities,

3 - evaluating the performance characteristics

of a number of available elements. The emphasis is placed on the linear flexural behavior of the most commonly used type of sandwich construction, namely the three layer symmetrical construction.

Chapter II includes a review of some fundamental equations in the analysis of sandwich plates. In this chapter, the structural behavior of sandwich plates and analytical solutions using equilibrium equations are discussed. Chapter III is a brief introduction to the formulation of the element stiffness matrices using displacement and assumed stress hybrid approaches.

Chapter IV deals with the displacement elements. In this chapter, characteristics of each element with regard to its geometric configuration, nodal degrees of freedom and capabilities are discussed. Chapter V contains a similar discussion for the assumed stress hybrid elements.

Chapter VI outlines the description of the numerical tests carried out for various hybrid elements in order to evaluate the convergence properties of each element as well as their accuracy for different aspect ratios and shear parameters.

Chapter VII is devoted to the discussion of the results for the hybrid elements. Chapter VIII includes the description of two new elements. The choice of stress functions and boundary displacements for these elements are discussed.

Finally, Chapter IX is a summary of the findings of this report and the conclusions.

CHAPTER II

SANDWICH PLATE THEORY

2.1 Governing Differential Equations for Sandwich Plates

Several theories have been developed for the analysis of three layer sandwich plates [3,29]. These theories entail various degrees of refinement regarding the stress distribution in the layers and inclusion of anisotropic materials in a given section. The following assumptions have been commonly adopted by these theories.

1. Displacements and strains are sufficiently small so that the linear theory of elasticity applies.
2. Transverse displacements at all points on a line normal to the mid-plane are the same.
3. Interlayer bonds are strong enough to prevent slippage between adjacent layers.
4. In the core, planes normal to the neutral plane remain plane but not necessarily normal after the deformation.

Assumption 1 is made in order to avoid mathematical complications

associated with geometric and material non-linearities. Based on this assumption, the membrane and bending stresses are treated independently. Assumption 2 implies that the transverse normal strains are negligible. Therefore, no compaction of the layers in the transverse direction is permitted. The effect of local bond failures on the behavior of the plate is ignored by assumption 3. Finally, assumption 4 restricts the normals to deform without warping and as a result, transverse shear strains are taken to be a constant through the thickness of the core. It should be noted that the neutral plane of the section coincides with the mid-plane of the core only for symmetrical sections.

The analytical solutions [29] which are presented for comparisor purposes in Chapter VII, are based on the following additional assumptions:

5. Faces are thin such that their flexural rigidities about their own mid-planes are negligible.

6. The core carries no in-plane normal stresses.

Assumption 5 implies that the faces act as membranes whereas assumption 6 excludes the contribution of the core to the bending stiffness of a section.

Fig.(2.1) shows the sign convention for stress resultants acting on a

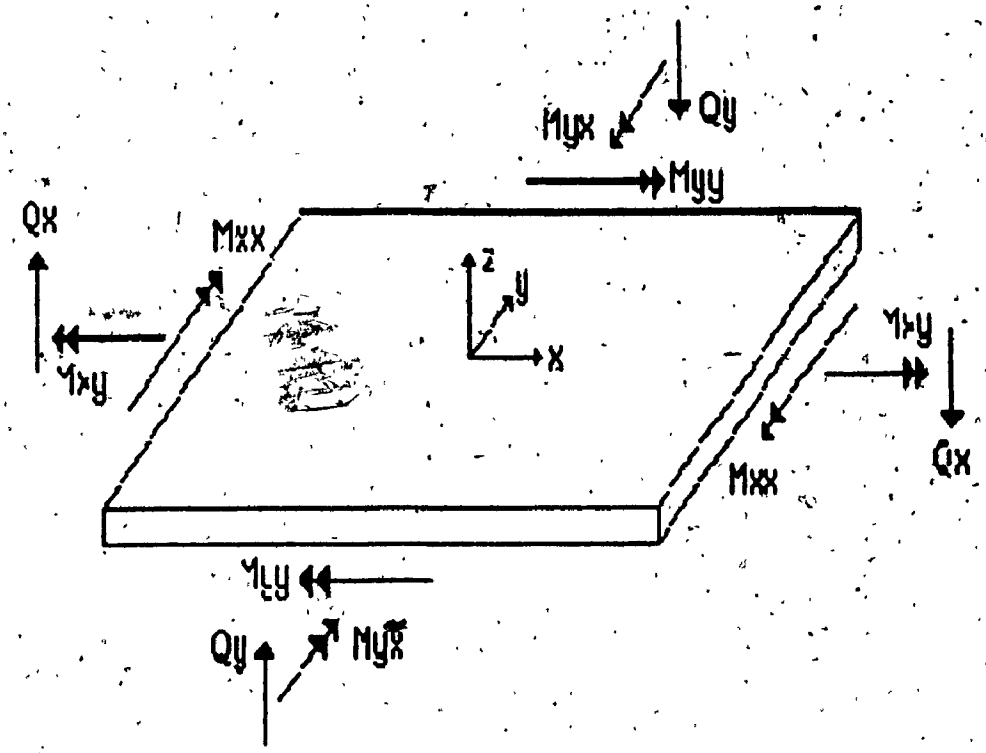

FIGURE 2.1: POSITIVE SIGN CONVENTION FOR STRESS RESULTANTS

segment of a three layer sandwich plate. It is noted that the equilibrium equations for sandwich plates remain identical to those of thin plate theory since the equations are in terms of stress resultants. These equations are [29]:

$$\partial M_{xx}/\partial x + \partial M_{xy}/\partial y - Q_x = 0 \qquad (2.1.1)$$

$$\partial M_{xy}/\partial x + \partial M_{yy}/\partial y - Q_y = 0 \qquad (2.1.2)$$

$$\partial Q_x/\partial x + \partial Q_y/\partial y - q = 0 \qquad (2.1.3)$$

where M_{xx}, M_{yy} are normal moments per unit length, M_{xy} is the twisting moment per unit length and Q_x, Q_y are the transverse shear forces per unit length. If all the above stresses act simultaneously on the plate segment of Fig.(1), then the resulting curvatures are given by Eq. (2.2) [29]:

$$w_{xx} = M_{xx}/B_x - \upsilon_y M_{yy}/B_y - \partial\gamma_x/\partial x \qquad (2.2.1)$$

$$w_{yy} = M_{yy}/B_y - \upsilon_x M_{xx}/B_x - \partial\gamma_y/\partial y \qquad (2.2.2)$$

where subscripts for w refer to its partial derivatives, γ_x and γ_y are the transverse shear strains and B refers to the stiffness of the section in bending. The last term in each of the above equations is the rate of change of transverse shear deformation which contributes to the curvature. The

negative signs are needed for the sign convention chosen. According to Betti's reciprocal theorem, B_x, B_y, υ_x and υ_y are interrelated and the relationship between them is:

$$B_x.\upsilon_y = B_y.\upsilon_x \qquad (2.3)$$

Eq.(2.2) can now be solved for M_{xx} and M_{yy} in terms of w_{xx}, w_{yy}, γ_x and γ_y. The resulting expressions are given in Eq. (2.4).

$$M_{xx} = D_x.[\partial(w_x+\gamma_x)/\partial x + \upsilon_y.\partial(w_y+\gamma_y)/\partial y] \qquad (2.4.1)$$

$$M_{yy} = D_y.[\partial(w_y+\gamma_y)/\partial y + \upsilon_x.\partial(w_x+\gamma_x)/\partial x] \qquad (2.4.2)$$

where:

$$D_x = B_x/(1-\upsilon_x.\upsilon_y) \qquad (2.4.3)$$

$$D_y = B_y/(1-\upsilon_x.\upsilon_y) \qquad (2.4.4)$$

The expression for M_{xy} is shown to be [29]:

$$M_{xy} = T.[\partial(w_x+\gamma_x)/\partial y + \partial(w_y+\gamma_y)/\partial x]/2 \qquad (2.5)$$

where T is the twisting stiffness of the section. Expressions for M_{xx}, M_{yy}, M_{xy} can now be substituted into Eq.(2.1) to obtain three differential equations in terms of w, γ_x and γ_y. For an isotropic sandwich plate, the

resulting expressions are much simpler and are given in Eq. (2.6).

$$\begin{bmatrix} \partial(\partial^2/\partial x^2+\partial^2/\partial y^2)/\partial x & \\ [\partial^2/\partial x^2+((1-\upsilon)\partial^2/\partial y^2)/2-S/D] & \\ [(1+\upsilon)\partial^2/\partial x\partial y]/2 & \end{bmatrix}^T . \{w,\gamma x,\gamma y\}^T = 0 \qquad (2.6.1)$$

$$\begin{bmatrix} \partial(\partial^2/\partial x^2+\partial^2/\partial y^2)/\partial y & \\ [(1+\upsilon)\partial^2/\partial x\partial y]/2 & \\ [((1-\upsilon)\partial^2/\partial x^2)/2+\partial^2/\partial y^2-S/D & \end{bmatrix}^T . \{w,\gamma x,\gamma y\}^T = 0 \qquad (2.6.2)$$

$$\partial\gamma_x/\partial x - \partial\gamma_y/\partial y - q/S = 0 \qquad (2.6.3)$$

where S is the shear stiffness of the section and:

$$\upsilon = \upsilon_x = \upsilon_y \qquad (2.6.4)$$

$$D = D_x = D_y \qquad (2.6.5)$$

$$S = S_x = S_y \qquad (2.6.6)$$

$$T = (1-\upsilon).D \qquad (2.6.7)$$

Equations (2.6.1) to (2.6.3) are the simultaneous governing equations for an isotropic sandwich plate. The solutions for w, γ_x and γ_y should satisfy the boundary conditions. At each supported edge, three conditions are

required instead of the two needed in thin plate theory. The boundary conditions for most common support types, at an edge with constant y, are as follows:

- Free: $M_{yy}=0 \; ; \; M_{yx}=0 \; ; \; Q_y=0$ (2.7.1)

- Simply supported: $w=0 \; ; \; M_{yy}=0$ (2.7.2)

- Clamped: $w=0 \; ; \; \partial w/\partial y + \gamma_y = 0$ (2.7.3)

The third condition for simply supported and clamped edges depends on the existence of the transverse shear strains at the edge. If shear strain is prevented at the support, then $\gamma_x = 0$. On the other hand, if shear strain γ_x is not prevented, then $M_{xy} = 0$. For the case of the clamped edge, the latter is a theoretical possibility which does not commonly occur in practice. For boundary conditions along an edge with constant x, the x and y's must be interchanged in the above expressions.

Fig. (2.2) shows the cross section of a three layer symmetric sandwich plate. The stiffness expression for this section can be derived noting the exact and assumed stress distribution in a section as shown in Fig. (2.3) by plain and solid lines respectively. The general expression for B for a segment of unit width of an isotropic symmetric three layer sandwich

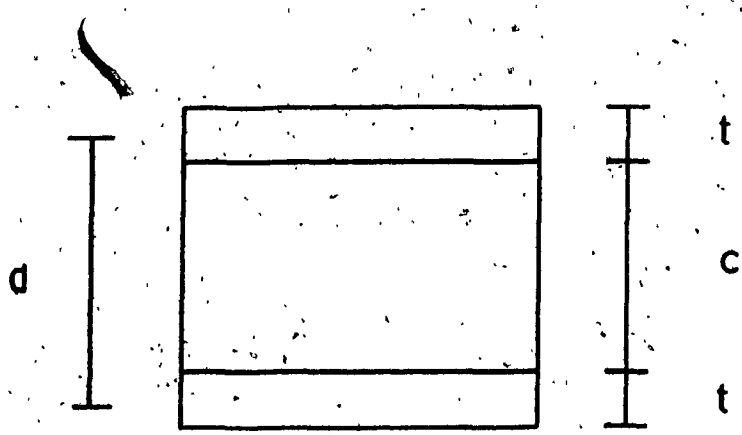

FIGURE 2.2: SECTION OF A SYMMETRIC THREE LAYER SANDWICH PLATE.

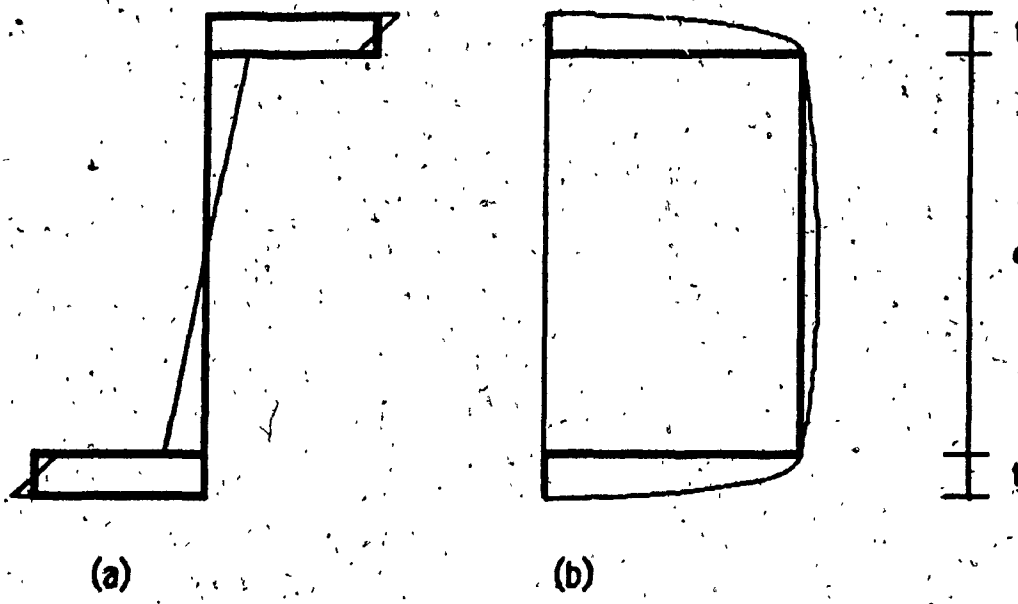

FIGURE 2.3: EXACT (PLAIN LINES) VS. ASSUMED (SOLID LINES) STRESS DISTRIBUTION IN A SECTION OF A SYMMETRIC THREE LAYER SANDWICH PLATE: (a) BENDING STRESSES, (b) TRANSVERSE SHEAR STRESSES.

plate is given by Eq. (2.8).

$$B = E_f.t^3/6 + E_f.t.d^2/2 + E_c.c^3/12 \qquad (2.8)$$

However, if ,as in the present case, it has been assumed that the thin faces act as membranes and the core carries no longitudinal stresses, then the first and the third terms in Eq. (2.8) can be neglected. Therefore, B is as given in Eq.(2.9).

$$B = E_f.t.d^2/2 \qquad (2.9)$$

In Eq. (2.8), it is noted that the first term is less than 1% of the second if:

$$(d/t)^2 > 33.33 \qquad (2.10)$$

and the third term is less than 1% of the second if:

$$(E_f/E_c).(t/c).(d/c)^2 > 16.67 \qquad (2.11)$$

Equations (2.10) and (2.11) are normally satisfied for the practical range of material and geometric properties used for sandwich plates. Therefore, the assumptions lead to reasonable approximation of the exact solution, thus are justifiable. The shear stiffness of the same section is given by either Eq. (2.12.1) or (2.12.2).

$$S = G.d \qquad (2.12.1)$$

$$S = G.c \qquad (2.12.2)$$

Eq. (2.12.1) represents the stiffness for a section for which Eq. (2.10) is satisfied. Eq. (2.12.2) is a more limiting case where the ratio of t to d is assumed to be very small. This is true for a section with very thin faces. In this case, faces act as membranes and carry no transverse shear stresses.

CHAPTER III

BACKGROUND TO FINITE ELEMENT FORMULATION

3.1 Introduction

As mentioned in Chapter I, two different approaches are commonly used for the formulation of the sandwich plate finite elements. These methods differ basically in the choice of the functional to be minimized. In the displacement method, the functional chosen is the total potential energy of the element, whereas in the assumed stress hybrid method, the functional to be minimized is the total complementary energy. The underlying theories for these methods are extensively covered in the literature [10, 25, 26, 34]. In the following sections, these methods are briefly outlined in order to illustrate their differences.

3.2 Displacement Method

In this method [10, 34], a displacement field is assumed over the entire element. This displacement field is related to the nodal degrees of freedom by means of shape functions as given in Eq. (3.1):

$$\{u\} = [N].\{d\} \tag{3.1}$$

where $\{u\}$ is the displacement field vector, $\{d\}$ is the nodal degrees of freedom vector and $[N]$ is the shape function matrix. Strains, $\{\epsilon\}$, can now be expressed in terms of nodal degrees of freedom by simply taking the appropriate derivatives of the shape functions (Eq. (3.2)):

$$\{\epsilon\} = [B].\{d\} \tag{3.2}$$

where $[B]$ is obtained by taking derivatives of $[N]$. Stresses, $\{\sigma\}$, are calculated from strains by applying the generalized Hooke's law (Eq. (3.3)):

$$\{\sigma\} = [E].\{\epsilon\} \tag{3.3}$$

where $[E]$ is the elasticity matrix. The strain energy density, U_0, is defined as:

$$U_0 = 1/2 .\{\sigma\}^T.\{\epsilon\} \tag{3.4}$$

By substituting Eq. (3.3) into (3.4) and noting that $[E]$ is symmetric:

$$U_0 = 1/2. \{\epsilon\}^T.[E].\{\epsilon\} \tag{3.5}$$

The strain energy for the element, U, is obtained by integrating U_0 over the volume of the element. Therefore:

$$U = \int_{\underline{V}} U_0 \, d\underline{V} \tag{3.6}$$

which after substitution from Eqs. (3.2) and (3.5) and noting that {d} is constant for an element, can be written as:

$$U = 1/2.\{d\}^T.\int_{\underline{V}} [B]^T.[E].[B]\, d\underline{V}.\{d\} \qquad (3.7)$$

The potential energy of the applied loads, ignoring body forces, is given in Eq. (3.8).

$$V = -\int_{\underline{S}} \{u\}^T.\{p\}\, d\underline{S} - \{d\}^T.\{P\} \qquad (3.8)$$

In Eq.(3.8), {p} is the vector of distributed applied loads and {P} is the vector of nodal forces. After substituting for {u} from Eq. (3.1), V can be written as:

$$V = -\{d\}^T.\int_{\underline{S}} [N]^T.\{p\}\, d\underline{S} - \{d\}^T.\{P\} \qquad (3.9)$$

The total potential energy of the element, Π, is given by:

$$\Pi = U + V \qquad (3.10.1)$$

or after substituting from (3.7) and (3.9):

$$\Pi = 1/2.\{d\}^T \int_V [B]^T.[E].[B]\, dV.\{d\} - \{d\}^T. \int_S [N]^T.\{p\} dS - \{d\}^T.\{P\} \quad (3.10.2)$$

According to the principle of minimum potential energy, at equilibrium Π must be stationary. Therefore, at equilibrium:

$$\partial\Pi/\partial\{d\} = 0 \quad (3.11.1)$$

which, after substituting from Eq. (3.10.2) becomes:

$$\int_V [B]^T.[E].[B]\, dV.\{d\} - \int_S [N]^T.\{p\}\, dS - \{P\} = 0 \quad (3.11.2)$$

or

$$[K].\{d\} - \{Q\} = 0 \quad (3.11.3)$$

where [K] is the element stiffness matrix and {Q} is the equivalent load matrix and:

$$[K] = \int_V [B]^T.[E].[B]\, dV \quad (3.12.1)$$

$$\{Q\} = \int_S [N]^T.\{p\}\, dS + \{P\} \quad (3.12.2)$$

The expression (3.12.2) could be expanded in a similar manner to include body forces. These have been left out in the present case for simplicity.

3.3 Assumed Stress Hybrid Method

In this method [25,26], stresses are assumed within the element such that they satisfy the differential equilibrium conditions. The stresses, $\{\sigma\}$, are functions of local coordinates and a set of independent constant coefficients as given in Eq. (3.13).

$$\{\sigma\} = [P].\{\beta\} \qquad (3.13)$$

In Eq. (3.13), $\{\beta\}$ is the vector of independent coefficients which are to be calculated and [P] is a matrix containing x and y terms. The strains are now expressed in terms of stresses:

$$\{\epsilon\} = [C].\{\sigma\} \qquad (3.14)$$

where [C] is the compliance matrix. The complementary strain energy density is given by:

$$U_0 = 1/2.\{\sigma\}^T.\{\epsilon\} \qquad (3.15)$$

and the complementary strain energy is obtained by integrating over the volume:

$$U = 1/2. \int_V \{\sigma\}^T.\{\epsilon\}\, dV \qquad (3.16)$$

After substituting Eq. (3.13) and (3.14) in Eq. (3.16) and noting that $\{\beta\}$ is constant for a given element, U becomes:

$$U = 1/2.\{\beta\}^T.\int_V [P]^T.[C].[P]\, dV.\{\beta\} \qquad (3.17.1)$$

$$= 1/2.\{\beta\}^T.[H].\{\beta\} \qquad (3.17.2)$$

where:

$$[H] = \int_V [P]^T.[C].[P]\, dV \qquad (3.17.3)$$

For a well formulated element, the symmetric [H] matrix is positive definite. Next, a displacement field along the element edges is assumed. This assumed displacement function along each edge is expressed in terms of nodal degrees of freedom on that edge (Eq. (3.18)):

$$\{u\} = [L].\{d\} \qquad (3.18)$$

where {u} is the displacement field along all edges, {d} is the vector of element degrees of freedom and [L] contains the interpolation functions. By choosing a suitable set of interpolation functions for [L], the compatibility along the element boundaries can be readily achieved. The stresses along the edges, {S}, are expressed in terms of {β} as follows:

$$\{S\} = [R].\{\beta\} \qquad (3.19)$$

where [R] is a function of coordinates along the boundaries. The

complementary potential energy due to these stresses, W, can now be calculated to be:

$$W = -\oint \{S\}^T.\{u\}\, ds \qquad (3.20.1)$$

$$= -\{\beta\}^T.\oint [R]^T.[L]\, ds.\{d\} \qquad (3.20.2)$$

$$= -\{\beta\}^T.[T].\{d\} \qquad (3.20.3)$$

where:

$$[T] = \oint [R]^T.[L]\, ds \qquad (3.20.4)$$

The total complementary potential energy, Π_C is given by:

$$\Pi_C = U + W \qquad (3.21.1)$$

$$= 1/2.\{\beta\}^T.[H].\{\beta\} - \{\beta\}^T.[T].\{d\} \qquad (3.21.2)$$

which should be stationary. Therefore:

$$\partial\Pi_C/\partial\{\beta\} = 0 \qquad (3.22.1)$$

or

$$[H].\{\beta\} - [T].\{d\} = 0 \qquad (3.22.2)$$

Therefore:

$$\{\beta\} = [H]^{-1}.[T].\{d\} \qquad (3.23)$$

The element stiffness matrix can now be obtained noting that:

$$W = -\{Q\}^T.\{d\} \qquad (3.24)$$

where {Q} is the nodal loads vector. From Eq. (3.20.3) and (3.24) it can be concluded that:

$$\{Q\} = [T]^T.\{\beta\} \qquad (3.25.1)$$

which after substituting from Eq. (3.23) becomes:

$$\{Q\} = [T]^T.[H]^{-1}.[T].\{d\} \qquad (3.25.2)$$

From comparison of Eq. (3.25.2) and (3.11.3), it is evident that:

$$[K] = [T]^T.[H]^{-1}.[T] \qquad (3.26)$$

Once the element stiffness matrices and equivalent nodal loads are known, the global displacements can be found in a similar fashion to that of displacement method. Once the displacements are known, stresses can be calculated from Eq. (3.13) and (3.23).

3.4 Comparison of Displacement and Hybrid Methods

From the derivation of the stiffness matrix in the displacement method, it is evident that the choice of the displacement field is extremely important. Certain restrictions apply to the choice of displacement field

for an element. In order to assure convergence, $\{u\}$ must be selected such that [10]:

1. States of constant strains and rigid body modes are presented,

2. Displacements and strains are continuous within the element,

From Eq.(3.11.1) it is noted that the total potential energy obtained using displacement elements is larger than the actual. For this reason, the displacement method generally results in overstiff models. Higher order elements are usually more flexible and therefore yield more accurate results. However, there are disadvantages associated with choosing complex displacement functions. First, from Eq.(3.1) it is seen that the number of unknown coefficients in the displacement function must be at least equal to the total number of element degrees of freedom. A higher order element requires more coefficients and therefore more degrees of freedom thereby increasing the computation time required for analysis. The second disadvantage is that a complex function may impose undesired continuities of high order derivatives across the element boundaries. For example in some plate bending elements, curvatures remain continuous across inter-element boundaries. Although this does not jeopardize the convergence properties of the element, it has the disadvantage of

misrepresenting the stresses at points where flexural stiffness of the adjacent elements are not the same or where there are discontinuities in the bending moment diagram eg. points of application of concentrated moments. Furthermore, for all displacement elements, stresses are calculated from strains which are calculated by taking the derivatives of the displacements (Eq. (3.2) and (3.3)). Therefore, in general, the stresses are approximated less accurately than the displacements.

In the derivation of the stiffness matrix for assumed stress hybrid elements, the only requirement for the stress functions is that the equilibrium (Eq. (2.1)) be satisfied within the element. The complexity of these functions depend on the number of β's chosen which is less sevgrely dependent on the total number of degrees of freedom in the element.

The displacement field along the edges should be chosen such that requirement 1 is satisfied. It is noted that in the case of assumed stress hybrid elements, the domain for the assumed displacement field is limited to the element edges. Consequently, it is easier to find a suitable displacement function which meets the above requirement (ie. constant strains and rigid body modes). Also, fewer degrees of freedom are needed for this shape function compared to a displacement element having

identical edge displacement modes.

CHAPTER IV

DISPLACEMENT ELEMENTS

In this chapter, the characteristics of several displacement elements for sandwich plates will be disscused.

4.1 Monforton and Schmidt

This element [20] is capable of representing three layer sandwich plates with laminated faces and orthotropic core. Laminates in each face can have different material properties and as a result piecewise homogeneous, orthotropic material can be modelled. The expression for the strain energy includes terms related to the bending of the faces about their own axes, in-plane displacements of the faces and the transverse shear deformations of the core. The in-plane strength of the core is assumed to be negligible. Since flexural rigidities of the faces about their own axes are taken into account, sandwich plates with thick faces can be analyzed using this element.

The element is rectangular and has 8 nodes, located at the 4 corners

of each face as shown in Fig. (4.1). At each node, there are 8 degrees of freedom corresponding to the in-plane displacements as follows:

$$\{d_m\}^T = \{ u,\ v,\ u_x,\ u_y,\ v_x,\ v_y,\ u_{xy},\ v_{xy} \} \qquad (4.1)$$

where u and v are the in-plane displacements in x and y directions respectively and the subscripts refer to partial derivatives. Also, for each pair of nodes on the same vertical line, there are 4 degrees of freedom representing the lateral deflection:

$$\{d_b\}^T = \{ w,\ w_x,\ w_y,\ w_z \} \qquad (4.2)$$

That is, these two nodes are coupled by the above degrees of freedom in compliance with assumption 2. Therefore, the element has a total of 80 degrees of freedom.

The shape functions used, allow for cubic variation of u, v and w. The transverse shear deformation and the associated strain energy in the core are expressed in terms of the membrane degrees of freedom (Eq.(4.3)) noting the continuity of the inplane displacements at the interlayer boundaries.

$$\gamma_x = (u_1-u_2)/c - (d_1+d_2).w_x/c - w_x \qquad (4.3.1)$$

$$\gamma_y = (v_1-v_2)/c - (d_1+d_2).w_y/c - w_y \qquad (4.3.2)$$

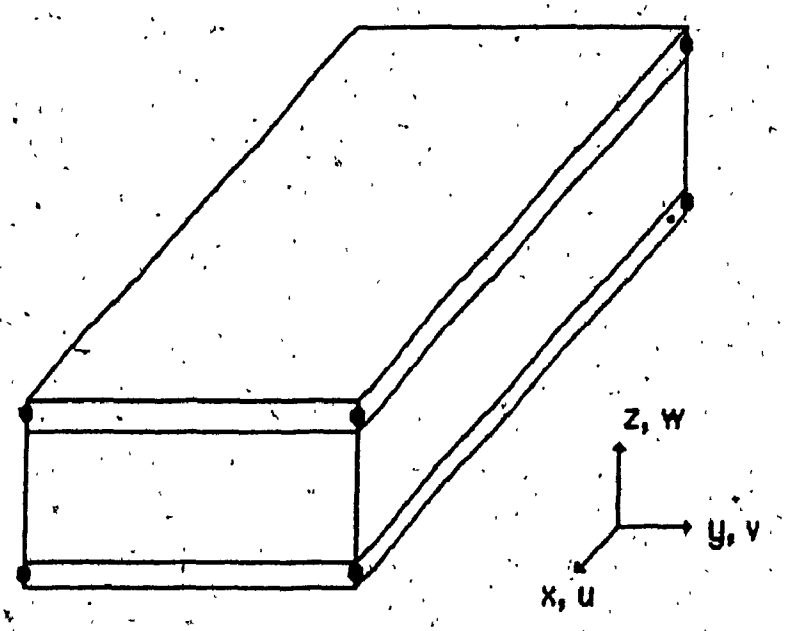

FIGURE 4.1: MONFORTON AND SCHMIDT'S ELEMENT

In the above equations, c is the core thickness, subscripts 1 and 2 refer to top and bottom surfaces respectively and d_1 and d_2 are the distances of the top and bottom neutral planes for the faces from the interlayer boundaries. For the case of a plate with homogeneous or symmetrically laminated faces d_1 and d_2 are equal to $t_1/2$ and $t_2/2$ respectively.

This element was tested on a square sandwich plate loaded uniformly in tension along two opposite edges with the other two opposite edges free. The exact results [31] were obtained because the assumed inplane displacement field is of the same order as the exact solution. In a second test, a simply supported square sandwich plate was subjected to a uniformly distributed load. The results for maximum deflection were identical to the analytical solution [16]. The errors for transverse shear strains at the mid-sides were less than 5.5% using 4 elements and less than 0.5% when using 16 elements.

The accuracy of the results obtained in the above tests are very good. However, as disadvantages of this element, one may mention the large number of degrees of freedom and the excessive continuity of the transverse shear strains in the core over inter-element boundaries at points of application of concentrated loads. Finally, the existence of

non-geometric degrees of freedom makes the element unsuitable for the analysis of systems such as folded plates and panelized buildings where the elements are joined at an angle. Also, for the same reason, such an element would unlikely be included in the element library of general structural analysis programs.

4.2 Ahmad, Irons and Zienkiewicz

These authors introduced a group of elements [1] suitable for the analysis of thin as well as thick plates or curved shells. For thick plates and shells, the effects of transverse shear deformation are included in the derivation of the element stiffness matrix. Even though these elements were only intended for the analysis of homogeneous plates, they can be adopted for sandwich plate analysis by suitable modification of the terms reflecting the bending and shear stiffnesses. These elements serve as a basis for some later sandwich plate elements. Basically, these elements are a reduced form of a parametric three dimensional solid element. However, transverse normal stresses and the corresponding strain energy are not taken into account in accordance with the plate bending theory. Also, in order to maintain the straightness of the normals after

deformation, the variation of the inplane displacements through the thickness is assumed to be linear.

These elements are hexahedral in shape and their number of nodes depends on the order of displacement functions required (Fig.(4.2)). However, only two nodes are needed through the thickness to ensure linear variation of inplane displacements. The degrees of freedom at each node are u, v and w. The two nodes lying on the same vertical line, share the same lateral deflection, w, in accordance with assumption 2. The energy due to transvese shear deformations is expressed in terms of γ_x and γ_y (Eq.(4.4)).

$$\gamma_x = \partial u/\partial z + \partial w/\partial x \qquad (4.4.1)$$

$$\gamma_y = \partial v/\partial z + \partial w/\partial y \qquad (4.4.2)$$

The capability of these elements to incorporate the effect of the transverse shear deformation in the behavior of a structure was tested on a water retaining tank with thin walls and a thick base. No analytical solutions exist for this problem and the results from another finite element analysis [2] were used as a benchmark for comparison. Equal number of elements were chosen for the model. The results using 15 cubic

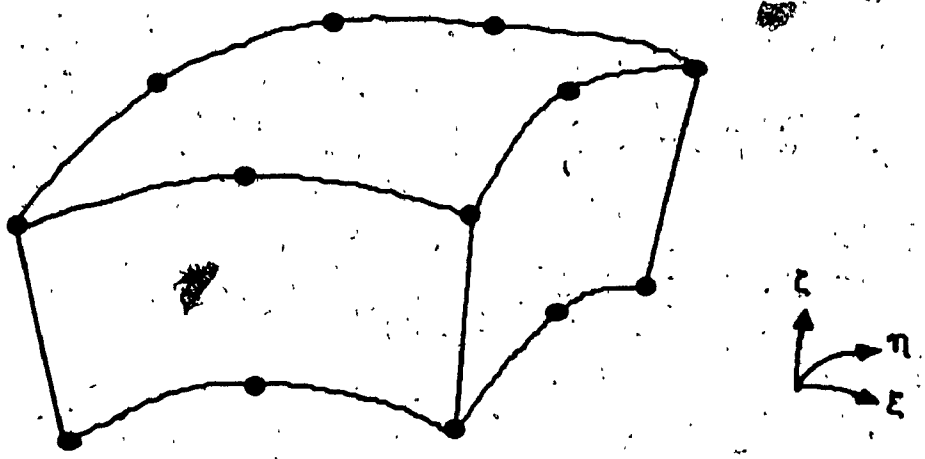

(a)

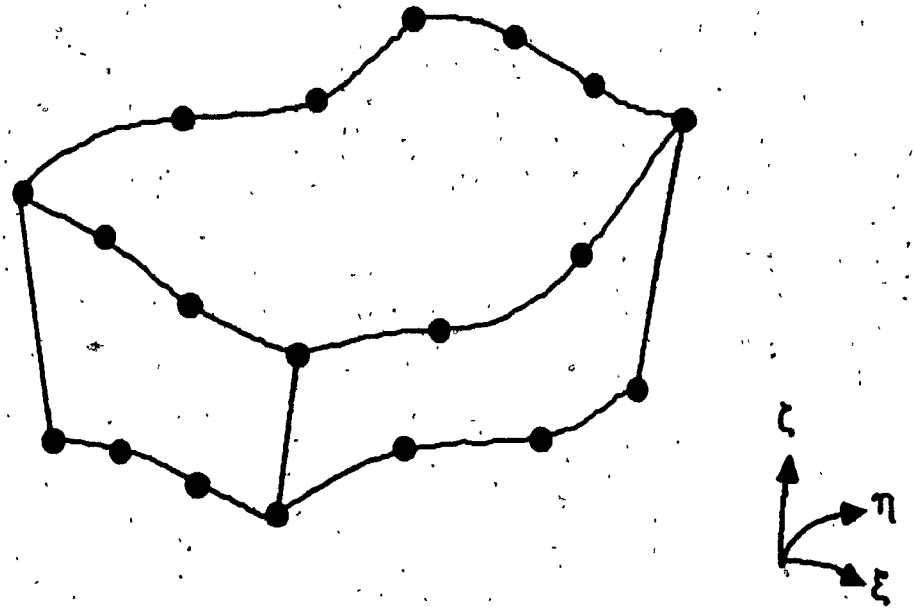

(b)

FIGURE 4.2: AHMA[illegible]LEMENT WITH (a) QUADRATIC AND (b) CUBIC SHAPE FUNCTIONS.

elements are in close agreement with the reference values. In another test, a thick clamped cicular plate subjected to uniformly distributed load was analyzed using cubic elements. The results for transverse displacements, radial and tangential stresses deviate little from analytical results [31].

This group of elements has a wide range of applicability as mentioned above. Furthermore, they can also be applied to the analysis of sandwich plates or shells if the elasticity matrix includes the equivalent material properties of the sandwich section as explained in Chapter II. In such a case, the stress resultants would be valid, and from which the stresses in each layer can be calculated. Finally, it is noted that the degrees of freedom for these elements are geometrical, making their implementation into existing finite element systems relatively easy. However, because of the large number of nodes and the three dimensional nature of these elements, their use for modelling panelized structures would pose serious problems.

4.3 Pryor and Barker

This element [30] is capable of including the effect of transverse shear deformations in an arbitrary laminated plate. Each layer can have

orthotropic material properties. The expression for the strain energy includes the energy due to the transverse shear deformation of each layer as well as the flexural rigidity of each laminate about its own axis. Thus for each layer, all stresses are assumed to be non-zero except for the transverse normal stress which is ignored according to assumption 2.

This element is rectangular with 4 corner nodes (Fig. (4.3)). At each node there are 7 degrees of freedom:

$$\{d\}^T = \{ u, v, w, \theta_x, \theta_y, \gamma_x, \gamma_y \} \qquad (4.5)$$

where θ_x and θ_y are the rotations of the normal about the x and y axis respectively. Also, γ_x and γ_y are the average values for the entire section and are used in the strain energy expression. Since the average values for the transverse shear strains are used, it is assumed that the total rotations of the normal at a given point are the same through the thickness. This is evident noting that:

$$\theta_x = w_x + \gamma_x \qquad (4.6.1)$$

$$\theta_y = w_y + \gamma_y \qquad (4.6.2)$$

Assuming an average value for all layers could lead to misrepresentation of

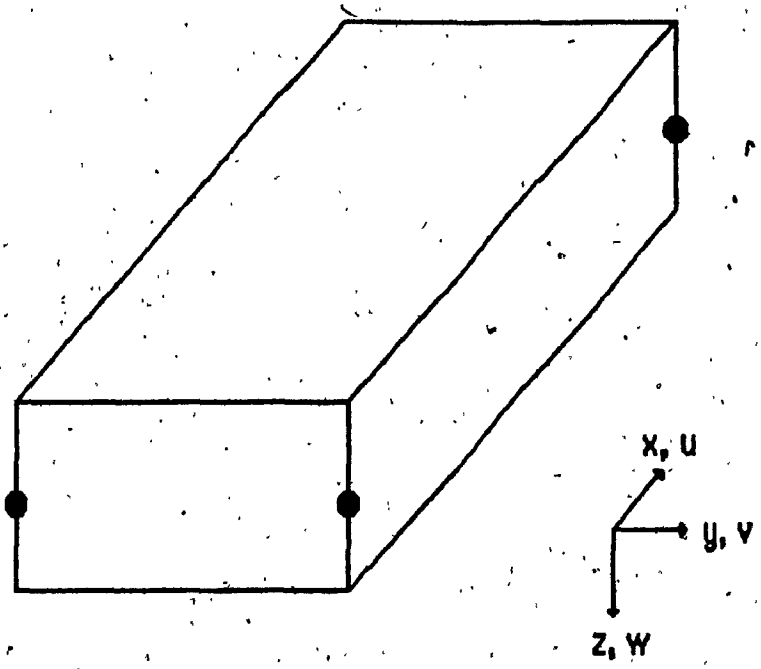

FIGURE 4.3: PRYOR AND BARKER'S ELEMENT

the actual shear strains and stresses especially where constituent layers possess significantly different material properties. This point has been acknowledged by the authors and as a remedy the transverse shear stresses are calculated from the elasticity equilibrium equations rather than from γ_x and γ_y.

This element was used to model a simply supported, square, symmetric crossply (0/90/90/0) laminate subjected to sinusoidal loading of the form $q_0.\text{Sin}\,(\pi x/a).\text{Sin}(\pi y/a)$. The non-dimensional results for the maximum deflection show good agreement with the analytical results [33]. Also, an infinitely long, simply supported, symmetric crossply (0/90/0) strip subjected to sinusoidal loading of the form $q_0.\text{Sin}(\pi x/a)$ was analyzed [23]. The rotation of the normal and in-plane non-longitudinal stresses were poorly approximated. The lack of accuracy can be explained by noting that in the actual deformed shape of the three layer laminate the rotation of the middle layer is significantly different from that of the top and bottom layers, whereas in the formulation of the element, the same rotation through the thickness has been assumed.

This element allows for anisotropic material properties in arbitrarily laminated plates and it has relatively few degrees of freedom.

However, its results seem to be more accurate when there are no severe discountinuities in the rotations of the normals in each layer. This limits the applicability of this element to cases where all layers have similar properties. To rectify this shortcoming, the above authors have suggested the use of seperate normal rotations for each layer. This suggestion was later implemented, details of which are given in the following sections.

4.4 Khatua and Cheung

This element [13] can represent multilayer flat sandwich plates where thin layers of high stiffness materials (faces) are separated by relatively thick layers of lower stiffness and density (cores). Orthotropic materials for faces and cores are included in the formulation. This element takes into account the strain energy due to bending and stretching of each face as well as transverse shear deformation of each core. Therefore, sandwich plates with thick faces can be properly modelled.

The element is triangular with 3 corner nodes and 3 mid-side nodes on each face (Fig.(4.4)). There are no nodes attached to the cores. The corner nodes, each have 5 degrees of freedom as follows:

$$\{d\}^T = \{ u, v, w, \theta_x, \theta_y \} \qquad (4.7)$$

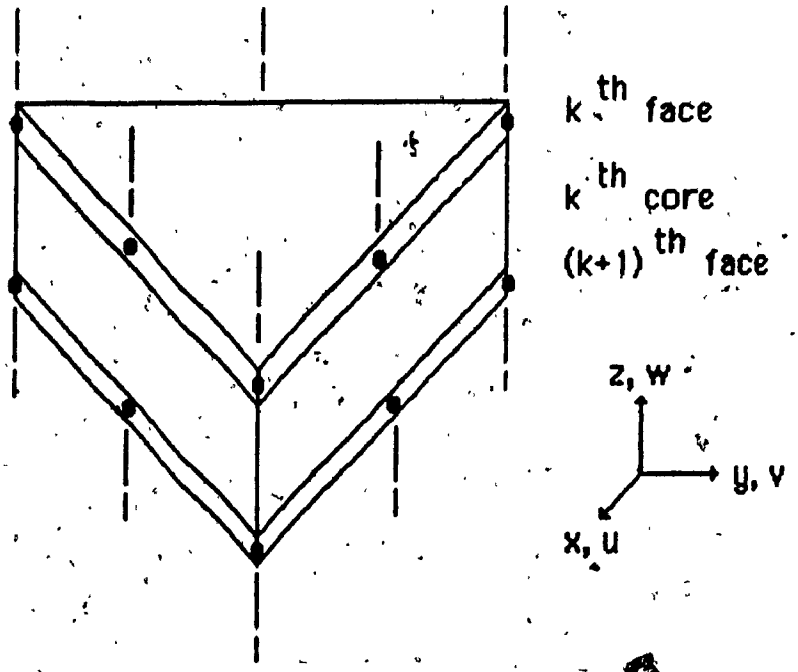

FIGURE 4.4: KHATUA'S TRIANGULAR ELEMENT

where the last three degrees of freedom are common to the nodes lying on the same vertical line according to assumption 2. The mid-side nodes, have 2 degrees of freedom each:

$$\{d\}^T = \{ u, v \} \qquad (4.8)$$

Therefore, the total number of degrees of freedom for a multilayer plate with n layers (ie. (n+1)/2 faces and (n-1)/2 cores) is 6*n+15.

The variation of w is cubic while that of u and v is quadratic. The transverse shear strain in each core is assumed to be constant according to assumption 4. These strains are expressed in terms of inplane displacements of the two neighboring faces as given in Eq. (4.9):

$$\gamma_{xj} = \left[(u_{i+1} - u_i)/d_j + \partial w/\partial x \right] . d_j/c_j \qquad (4.9.1)$$

$$\gamma_{yj} = \left[(v_{i+1} - v_i)/d_j + \partial w/\partial y \right] . d_j/c_j \qquad (4.9.2)$$

where d_j is the distance between the middle of the two adjacent faces. These equations can be easily derived noting the continuity of u and v at the interlayer boundaries.

A similar element [14] has also been developed which is rectangular.

This element has only 4 corner nodes on each face (Fig.(4.5)). The degrees of freedom at each node are given by Eq.(4.7). Therefore, an element with n layers has 4*n+16 degrees of freedom. The variation of w follows a 12 term polynomial whereas that of u and v is bilinear in x and y. The range of application of this element is identical to that of the triangular element.

The accuracy of these elements was investigated in numerical examples involving a three layer, simply supported, square sandwich plate subjected to uniformly distributed load. Two cases of isotropic [17] and orthotropic [4] faces were considered. The results for the central deflection and bending moments were compared with the analytical solutions. The analytical result for bending moment for the orthotropic case was not provided by the reference. The remaining test results show good agreement with the analytical solutions.

A similar example was considered with a five layer sandwich plate [4,17]. Once more, the accuracy of the elements are acceptable. The rectangular element was also used to model a three layer, clamped square sandwich plate subjected to uniform pressure [29]. A close match between analytical and test results is observed. For the common examples, the rectangular element required a larger number of elements than triangular

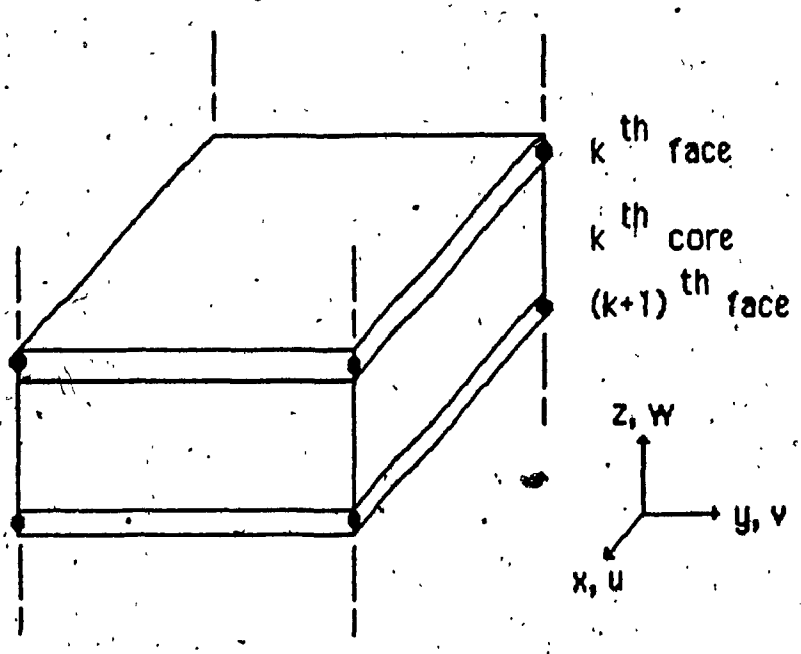

FIGURE 4.5: KHATUA'S RECTANGULAR ELEMENT

elements to achieve the same order of accuracy. This is not surprising since the rectangular element has fewer degrees of freedom than the triangular element.

These elements can be applied to a wide range of orthotropic multilayer sandwich plates with thick faces. Their advantage lies in the fact that in the derivation of the stiffness matrix, specific deformed shape of sandwich plates (ie. constant transverse shear in the cores) has been utilized in order to reduce the number of element degrees of freedom. In fact, these elements have fewer degrees of freedom than the corresponding composite laminate element. Also, these elements have inplane degrees of freedom. Therefore, they can, after some modifications, be used as flat shell elements. Finally, it should be noted that although all degrees of freedom are geometrical, the 3-D nature of this element prevents its application to panelized buildings.

4.5 Mawenya and Davies

This element [19] is capable of representing an arbitrary laminated flat or curved plate. The formulation is parametric, thus making the modelling of curved boundaries possible. Each layer can have homogeneous,

orthotropic properties. In the formulation, it is assumed that any layer may undergo transverse shear deformation and that each layer contributes to the flexural rigidity of the laminate. Therefore, the element can cover a wide range of material and geometric properties.

This element is based on Ahmad's parametric element. Its shape is hexahedral with 4 corner nodes and 4 mid-side nodes on each layer (Fig.(4.6)). A plane in the first layer is specified as the reference plane. The nodes on the first layer are located on the reference plane and have 5 degrees of freedom each (Eq. (4.7)). The nodes on any other layer have 2 degrees of freedom each:

$$\{d\}^T = \{ \theta_x, \theta_y \} \qquad (4.10)$$

Therefore, a plate consisting of n layers has a total of 16*n+24 degrees of freedom.

The variation of u, v and w is an incomplete cubic. For each layer, ϵ_{zz} is assumed to be zero according to assumption 2. The energy corresponding to the inplane displacements is expressed in terms of u and v for a reference layer as well as θ_x and θ_y of layers 1 through (I-1). The appropriate expressions are derived noting the continuity of inplane

displacements at the interlayer boundaries. The transverse shear strains are also expressed in terms of nodal degrees of freedom:

$$\gamma_{xj} = \theta_{xj} - w_x \qquad (4.11.1)$$

$$\gamma_{yj} = \theta_{yj} - w_y \qquad (4.11.2)$$

Numerical examples identical to that of Khatua's [13,14] have been carried out on this element. The results were compared with the same references [4,17]. The accuracy of the results, for a reasonable mesh size, is quite good. The element was also tested on a 3 layer, clamped, circular sandwich plate [29] in order to demonstrate its ability to handle curved boundaries. Other tests include a 3 layer, symmetric, simply supported rectangular sandwich plate and a similar 5 layer square plate subjected to sinusoidal loading [22,24]. Different width to thickness ratios were considered. For the above test problems, the results show, once more, good agreement with the analytical solutions.

This element is suitable for modelling of orthotropic multilayer composite laminates. The parametric formulation simplifies the modelling of curved edges. Also, the performance of the element, based on the given numerical tests, seem to be quite reliable. However, this element has a

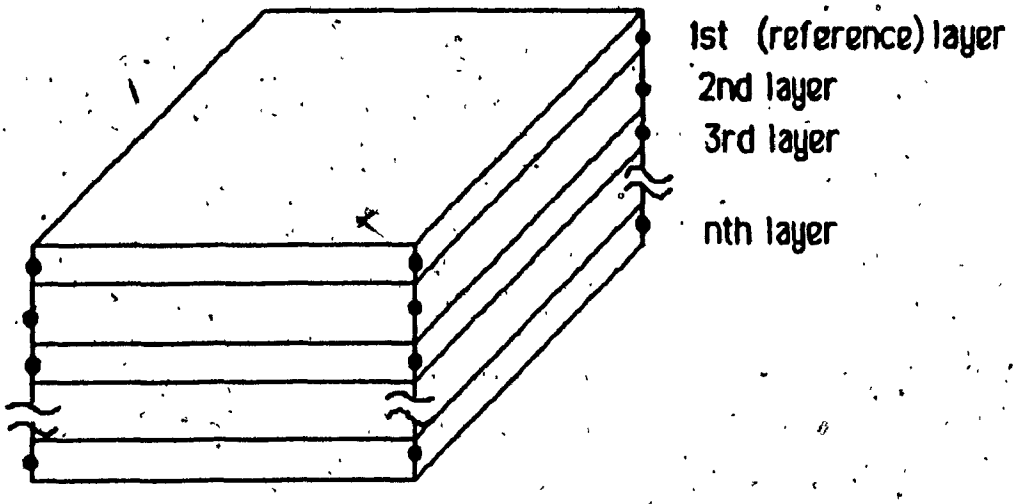

FIGURE 4.6: MAWENYA AND DAVIES'S ELEMENT

large number of nodes and degrees of freedom. The excessive number of degrees of freedom make this element undesirable for application to sandwich plates because many of degrees of freedom become, not surprisingly, redundant. Furthermore, due to its 3-D nature, this element cannot be used for the analysis of panelized structures.

4.6 Panda and Natarajan

This element [21] is capable of representing an arbitrary layered plate. Material for each layer can be homogeneous orthotropic. The strain energy associated with transverse shear strains and inplane displacements of each layer are taken into account.

The element is quadrilateral and has 4 corner and 4 mid-side nodes (Fig.(4.7)). At each node there are 5 degrees of freedom as given by Eq.(4.7). Each layer is considered to be in a specific three dimensional stress state with ϵ_{zz} assumed negligible according to assumption 2. The strains in each layer are expressed in terms of the above degrees of freedom. It is noted that the same rotations and therefore the same transverse shear strains have been assumed through the thickness of the laminate. The different material properties of each layer is taken into

account by piecewise integration over the thickness in this superparametric element.

The performance of this element was evaluated on four numerical examples. The first example was a three layer (0/90/0) simply supported square plate [24]. In the second example, the square plate was replaced by a rectangle with aspect ratio of 3 [22]. For the above tests, a transverse sinusoidal load of intensity $q_0.Sin(\pi x/a).Sin(\pi y/b)$ was applied on the structure. The other two examples, were identical to those considered by Pryor and Barker [30]. The test results were compared to analytical solutions [23,33] in all cases and also to results obtained by Mawenya's element [19] for the first and second examples.

In the first and second examples, the results agree fairly well with the exact analytical solutions. In these cases, the displacement results are stiffer than those of Mawenya's element and are generally more accurate. The accuracy of results for displacements and stresses are better for larger width to thickness ratios. This is expected because transverse shear strains, which are assumed to be constant for all layers in a section, are more significant for lower width to thickness ratios. Results for examples 3 and 4, also approximate the exact analytical solutions closely.

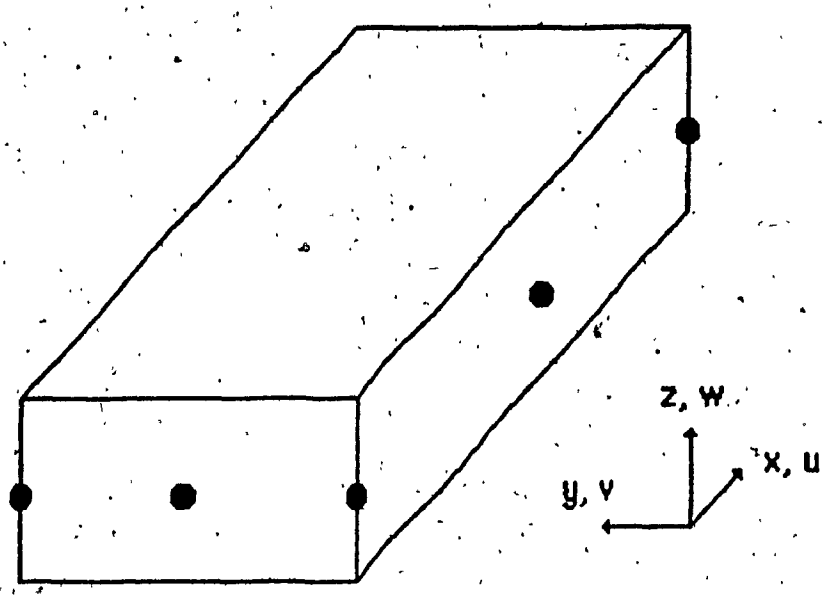

FIGURE 4.7: PANDA AND NATARAJAN'S ELEMENT

This element is suitable for modelling multilayer orthotropic composite laminates. It has the capability of representing curved boundaries. Its performance, based on the results from the numerical tests, is quite good. This element has the advantage of having only 40 degrees of freedom regardless of the number of layers in the laminate. The fewer degrees of freedom is achieved by assuming constant transverse shear deformation through the thickness. Therefore, some of the shortcomings of Pryor's element [30], as mentioned in section 4.3, are retained.

4.7 Summary

From the discussion of the preceeding sections, it can be concluded that Khatua's elements [13,14] are more suitable for the analysis of sandwich plates than the other elements. These elements have been based on the assumptions listed in Chapter II and their degrees of freedom has beeen accordingly chosen. Furthermore, these elements, which are capable of representing multilayer orthotropic sandwich plates with thick faces, have proven to be accurate in a number of numerical examples [13,14].

Panda's element [21] is more suitable than the other elements for the

analysis of orthotropic composite laminates. This element has fewer degrees of freedom compared to elements with similar capabilities and it is quite accurate. However, a common normal rotation through the thickness has been assumed. Therefore, the application of this element, as intended, is limited to cases where this assumption is valid. In other cases, the use of Mawenya's element should be considered. This element can also be used to model multilayer orthotropic composite laminates. However, separate normal rotations have been assumed for each layer.

The advantage of the latter two elements over the Monforton's [20] and Pryor's [30] elements is the efficient use of degrees of freedom. Monforton's element has 80 degrees of freedom including first and second derivatives of inplane displacements. Pryor's element has only 28 degrees of freedom but these include w, γ as well as θ at each node. These degrees of freedom are not independent as indicated by Eq.(4.6).

Finally, it should be emphasized that none of the elements discussed are suitable for modelling of sandwich panelized buildings because of the existence of non-geometrical degrees of freedom, or the 3-D nature of the element itself, or the exclusion of the effects of significant transverse shear deformations in the core.

CHAPTER V

HYBRID ELEMENTS

5.1 Introduction

Hybrid elements were introduced by Pian in 1964 [25]. The most common type of these elements are assumed stress hybrid elements. For this group of elements, one assumes a set of self-equilibrating stresses within the element and simultaneously, independent boundary displacements so that inter-element compatibility is maintained. In this study, the focus will be on those elements which are capable of representing symmetric, three layer, flat sandwich plates subjected to transverse loading.

In deriving the stiffness matrix for these elements, assumptions 1 through 4 of Chapter II are adopted. Assumption 1, regarding the linear behavior of the element, is incorporated in the choice of constant [C] in Eq. (3.14). Assumption 2 which imposes zero noraml transverse strain, is maintained by excluding ϵ_{zz} from $\{\epsilon\}$, thus neglecting the associated strain energy. Assumption 3 which disallows relative slippage of adjacent layers, is implicitly made in Eq. (3.16) where it is assumed that no strain energy is

lost through this type of deformation. Assumption 4, regarding the non-normality of the planes after deformation, is reflected in the choice of w, θ_x and θ_y as the degrees freedom. It is noted that according to Eq. (4.6), θ_x and θ_y include rotation of the normal due to shear. Associated with transverse shear deformations are shear resultants, Q_x and Q_y, which are also assumed within the element. The strain energy due to transverse shear deformations is then expressed in terms of Q_x, Q_y, γ_x and γ_y.

Since stress resultants rather than stresses are assumed, the assumptions 5 and 6 can be easily incorporated through proper choice of B and S. Similarly, sections including layers with orthotropic material properties can be modelled by using the appropriate expressions for B and S. This is an added advantage of sandwich plate bending hybrid elements over displacement elements for which a corresponding extension of capabilities usually would require major revisions of the element formulation. Furthermore, for these elements, only w, θ_x and θ_y are needed as degrees of freedom at each node. This is due to the fact that for assumed stress hybrid plate bending elements, only compatibility of

transverse displacements and rotations is required between neighboring elements and for these elements, displacements are prescribed only along the edges. Another advantage of using hybrid elements is that, due to their 2-D nature and their geometrical degrees of freedom, a flat shell element can be easily developed from a plate bending element. This can be achieved by simply augmenting the stiffness matrix of the plate bending element by the stiffness matrix of an assumed stress hybrid membrane element of the same geometry. The resulting flat shell element can be used to analyze three dimensional panelized structures [11,15].

From Section 3.3, it is apparent that a number of hybrid elements can be formulated using various combinations of stress functions and boundary displacements. However, it has been reported [27,28] that a necessary condition for an element to perform satisfactorily is :

$$m \geq n - r \qquad (5.1)$$

where m is the number of independent stress parameters, n is the number of element degrees of freedom and r is the number of rigid body modes. If Eq.(5.1) is not satisfied, then it is possible to find {d}, other than the rigid body modes, in Eq.(3.23) such that $\{\bar{\beta}\}$ becomes zero. Such solutions correspond to deformed shapes for the element which have zero strain

enery. In other words, the element becomes kinetically unstable. It should emphasized that Eq. (5.1) is not a sufficient condition for acceptable performance of an element for reasons which will be investigated later.

The next section includes descriptions of several hybrid elements. For each element, the assumed stress functions and prescribed edge displacements are presented.

5.2 Pian

Pian has developed a number of plate bending elements based on assumed stress hybrid formulation [25,26,27]. Most of these elements are suitable only for thin homogeneous plates and are not readily applicable to sandwich plates. In the formulation of these elements, the first derivatives of displacements were taken as degrees of freedom contrary to assumption 4. Modifications to some of these elements have been carried out by Krishnan [15] and will be discussed in Section 5.7.

Pian has briefly considered a rectangular element with 4 corner nodes [27]. At each node, three degrees of freedom are assigned as follows:

$$\{d\}^T = \{ w, \theta_x, \theta_y \} \qquad (5.2)$$

The assumed stresses are of the form:

$$M_{xx} = \beta_1+\beta_2x+\beta_3y+\beta_{10}x^2+\beta_{11}xy+\beta_{12}y^2 \qquad (5.3.1)$$

$$M_{yy} = \beta_4+\beta_5x+\beta_6y+\beta_{13}x^2+\beta_{14}xy+\beta_{15}y^2 \qquad (5.3.2)$$

$$M_{xy} = \beta_7+\beta_8x+\beta_9y+\beta_{16}x^2+\beta_{17}xy+\beta_{18}y^2 \qquad (5.3.3)$$

The expression for shear resultants are obtained by substituting Eq. (5.3) in Eq. (2.1). In doing so, it is noted that only 17 of the 18 β's are independent. The variation of displacements along the edges is taken to be linear and is given by:

$$w = (1-\xi)w_i + \xi w_j \qquad (5.4.1)$$

$$\theta_x = (1-\xi)\theta_{xi} + \xi\theta_{xj} \qquad (5.4.2)$$

$$\theta_y = (1-\xi)\theta_{yi} + \xi\theta_{yj} \qquad (5.4.3)$$

where subscripts i and j refer to the values at nodes i and j and ξ is the normalized coordinate along ij (Eq.(5.5)).

$$\xi = s / L_{ij} \qquad (5.5)$$

where s is the actual distance of a given point on side ij from node i and L_{ij} is the length of side ij. Similar elements have been considered by Ha [11]

and Barnard [15] as described in sections 5.5 and 5.6 respectively.

5.3 Bartelds and Ottens

This element [6] is triangular and has 6 nodes, three at the vertices and three at the mid-sides. At each node there are 3 degrees of freedom as given by Eq. (5.2). The moment distribution for this element is given by Eq. (5.3). Therefore, this element has also 17 independent stress parameters. The variation of displacements and rotations along each side is parabolic as given in Eq. (5.6).

$$w = (2\xi^2-3\xi+1)w_i + (-4\xi^2+4\xi)w_m + (2\xi^2-\xi)w_j \qquad (5.6.1)$$

$$\theta_x = (2\xi^2-3\xi+1)\theta_{xi} + (-4\xi^2+4\xi)\theta_{xm} + (2\xi^2-\xi)\theta_{xj} \qquad (5.6.2)$$

$$\theta_y = (2\xi^2-3\xi+1)\theta_{yi} + (-4\xi^2+4\xi)\theta_{ym} + (2\xi^2-\xi)\theta_{yj} \qquad (5.6.3)$$

where subscript m refers to the value at the mid-side node and all other variables are the same as in section 5.2.

5.4 Cook

Cook has introduced a family of triangular elements with 3 corner nodes [7,8]. At each node there are 3 degrees of freedom as given in Eq.

(5.2). These elements have 5, 7 and 9 independent stress parameters. The moment distribution for these elements are given in Eq.(5.7), (5.8) and (5.9) respectively.

$$M_{xx} = \beta_1 + \beta_4 x \qquad (5.7.1)$$

$$M_{yy} = \beta_2 + \beta_5 y \qquad (5.7.2)$$

$$M_{xy} = -\beta_3 \qquad (5.7.3)$$

$$M_{xx} = \beta_1 + \beta_4 x + \beta_6 y \qquad (5.8.1)$$

$$M_{yy} = \beta_2 + \beta_5 x + \beta_7 y \qquad (5.8.2)$$

$$M_{xy} = \beta_3 \qquad (5.8.3)$$

$$M_{xx} = \beta_1 + \beta_4 x + \beta_7 y \qquad (5.9.1)$$

$$M_{yy} = \beta_2 + \beta_5 x + \beta_8 y \qquad (5.9.2)$$

$$M_{xy} = \beta_3 + \beta_6 x + \beta_9 y \qquad (5.9.3)$$

The variation of rotations along the edges is linear and is given by Eq. (5.4.2) and (5.4.3). The variation of w is quadratic and depends on the

tangential rotations along the edge. The expression for the edge shape function used is:

$$w = (1-\xi)w_i + \xi w_j + L_{ij}\xi(1-\xi)(\theta_i - \theta_j)/2 \qquad (5.10)$$

where θ is the tangential rotation along the edge and the remaining variables are as defined in section (5.2).

5.5 Ha

Ha has developed two assumed stress hybrid elements [11]. The first is a rectangular element with 4 corner nodes and the second is a right angled triangular element with 3 corner nodes. The nodal degrees of freedom for these elements are given by Eq. (5.2). The assumed stress field for these elements is given by Eq. (5.3). The variation of displacements and rotations along the edges is given by Eq. (5.4). In the numerical tests of Chapter VI, only the rectangular element has been considered as this element's performance is reported to be superior to that of the triangular one [11].

5.6 Barnard

Barnard has introduced a quadrilateral and a triangular element having 4 and 3 corner nodes respectively [5]. The degrees of freedom at each node are given by Eq. (5.2). The stress distribution for this element is given by Eq. (5.3). The displacement field along the edges is given by Eq. (5.4).

The quadrilateral element in its rectangular form is different from Ha's element in only the choice of expression for S. For this element, S is given by Eq.(2.13.2) whereas Eq.(2.13.1) is used in Ha's element. For the numerical examples considered in Chapter VI, very thin faces are assumed and this difference is of no consequence. Therefore, only Ha's rectangular element [11] has been considered in the numerical tests.

5.7 Krishnan

Krishnan has considered a group of rectangular elements with 4 corner nodes [15]. The degrees of freedom at each node are give by Eq. (5.2). Therefore, each element has 12 degrees of freedom. Four different stress fields have been considered. Three of these with 5, 7 and 9 independent stress parameters are given by Eq. (5.7), (5.8) and (5.9)

respectively. The fourth distribution has 11 independent parameters and is given by:

$$M_{xx} = \beta_1+\beta_4x+\beta_7y+\beta_{10}xy \qquad (5.11.1)$$

$$M_{yy} = \beta_2+\beta_5x+\beta_8y+\beta_{11}xy \qquad (5.11.2)$$

$$M_{xy} = \beta_3+\beta_6x+\beta_9y \qquad (5.11.3)$$

The displacement and rotations vary linearly along the boundaries according to Eq. (5.4).

5.8 Zero Energy Modes

For ease of reference, the hybrid elements to be discussed will be referred to as Rm or Tm. The letter "R" or "T" refer to rectangular or triangular elements respectively and the letter "m" designates the number of stress parameters. For elements with mid-side nodes, "m" is followed by "-" and the number of mid-side nodes in the element. For example, R11 refers to a rectangular element with 11 β's and T17-3 refers to a triangular element with 17 β's and 3 mid-side nodes.

An unrestrained element stiffness matrix is in general singular and has a number of zero eigenvalues. The eigenvectors corresponding to zero

eigenvalues represent modes for which potential energy of edge forces is zero. For a well formulated element, these eigenvectors represent only the rigid body modes. For these elements, the stiffness matrix can be made non-singular if constraints are imposed to prevent rigid body modes.

For hybrid elements, it has been shown that it is possible to have a singular stiffness matrix even if the rigid body modes have been suppressed [9,27]. In such cases, the number of zero eigenvalues of the element stiffness matrix is more than the number of rigid body degrees of freedom. The eigenvectors corresponding to these additional zero eigenvalues represent deformed shapes for which the potential energy of edge forces is zero. These deformed shapes are known as zero energy modes and are presented by the additional eigenvectors.

For hybrid elements under consideration, the potential energy of the edge forces is given by Eq. (5.12).

$$W = \int\int_A \{ - M_{xx} . \theta_{y,x} - M_{xx,x} . \theta_y + M_{yy,y} . \theta_x + M_{yy} . \theta_{x,y} \} dxdy +$$

$$\int\int_A \{ + M_{xy} . \theta_{x,x} + M_{xy,x} . \theta_x - M_{yx} . \theta_{y,y} - M_{yx,y} . \theta_y \} dxdy +$$

$$\int\int_A \{ - Q_x . w_{,x} - Q_{x,x} . w - Q_y . w_{,y} - Q_{y,y} . w \} dxdy \qquad (5.12)$$

where ,x and ,y refer to partial derivatives of a function. If the mathematical expression for zero energy modes along with the appropriate expressions for the stress distribution are substituted in the right hand side of Eq. (5.12), both integrals will vanish. However, it is not always possible to obtain the exact mathematical expression for the zero energy modes. It is noted that W in Eq. (5.12) vanishes for any stress distribution if constant w, θ_x or θ_y are substituted in the right hand side. This is expected since these expressions correspondto the rigid body modes for an element.

The existence of zero energy modes could adversely affect the accuracy of an element if in a given mesh, adjacent elements can simultaneously assume zero energy deformed shapes. Therefore, it is

necessary to suppress these modes. However, for some zero energy modes, due to geometric compatibility requirements, this problem does not exist. The accuracy of an element is not affected by these modes. All zero energy modes can be suppressed if a sufficient number of independent stress parameters are chosen. The required complexity of the stress field, in order to suppress zero energy modes, depends on the mathematical expressions for these modes. These mathematical expressions are in general difficult, if not impossible, to obtain. Therefore, it is often not possible to predetermine the necessary terms in the stress fields for eliminating all zero energy modes.

Among the elements considered earlier, elements R23, R17 and R11 have no zero energy modes. Elements T5, T7 and T9 have one zero energy mode each. The zero energy mode for these elements is shown in Fig. (5.1). By inspection of Eq. (5.12), the expression for this mode is found to be:

$$w = 0 \qquad (5.13.1)$$

$$\theta_x = Cx \qquad (5.13.2)$$

$$\theta_y = Cy \,. \qquad (5.13.3)$$

where C is a constant. It is noted that once Eq. (5.13) along with the stress

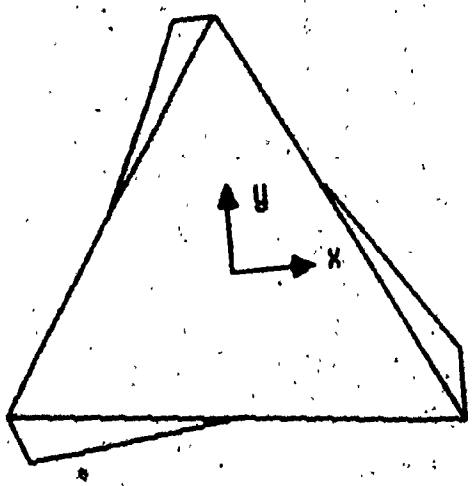

FIGURE 5.1: ZERO ENERGY MODE FOR T5, T7 AND T9

functions for T5, T7 or T9, represented by Eqs. (5.7), (5.8) and (5.9) respectively, are substituted in Eq.(5.12), zero W is obtained. This mode does not occur in a mesh because adjacent elements cannot assume the deformed shape of Fig.(5.1) simultaneously. It can also be noted that, in this case, if xy term is added to expressions for M_{xx} and M_{yy} in Eq. (5.7), (5.8) and (5.9), this zero energy mode vanishes.

Elements R7 and R9 have two zero energy modes each. The first mode is shown in Fig. (5.2a) and is similar to the mode for T5, T7 and T9. Once more, this mode can be suppressed by addition of xy term to the expressions for M_{xx} and M_{yy}. The second mode is shown in Fig. (5.2b).

Element R5 has four zero energy modes, two of which are identical to those of R7 and R9 (Fig.(5.2)). The third and fourth modes are given by Eq.(5.14) and (5.15) respectively.

$$w = 0 \qquad (5.14.1)$$

$$\theta_x = Cxy \qquad (5.14.2)$$

$$\theta_y = 0 \qquad (5.14.3)$$

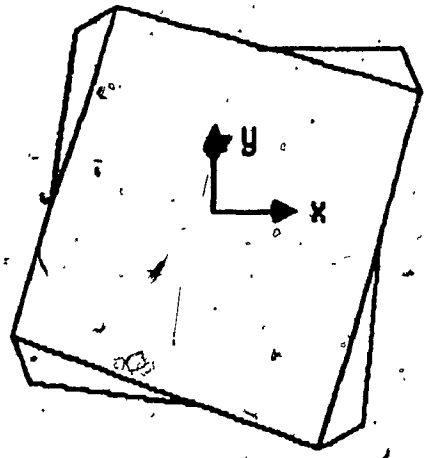

(a)

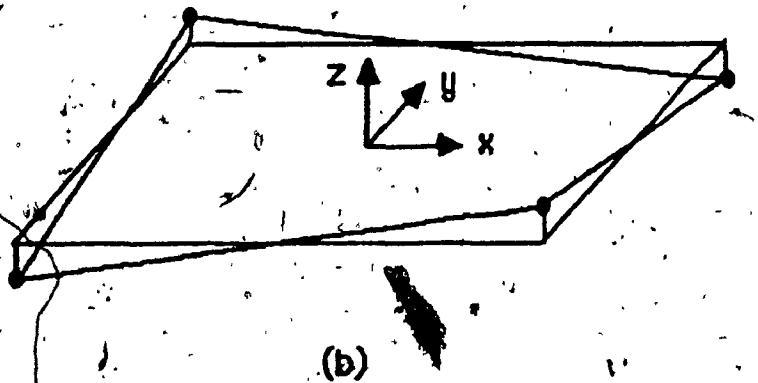

(b)

FIGURE 5.2: ZERO ENERGY MODES FOR R5, R7, R9

$$w = 0 \tag{5.15.1}$$

$$\theta_x = 0 \tag{5.15.2}$$

$$\theta_y = Cxy \tag{5.15.3}$$

where C is a constant. Zero W is obtained if Eq.(5.14) or (5.15) along with Eq.(5.7) is substituted in Eq.(5.12). These two modes can be suppressed if y and x terms are added to expressions for M_{xx} and M_{yy} in Eq.(5.7) respectively. The outcome would be identical to element R7 which has only two zero energy modes. Element T17-3 has only one zero energy mode as shown in Fig.(5.3). This mode may occur in a mesh and therefore, could distort the results.

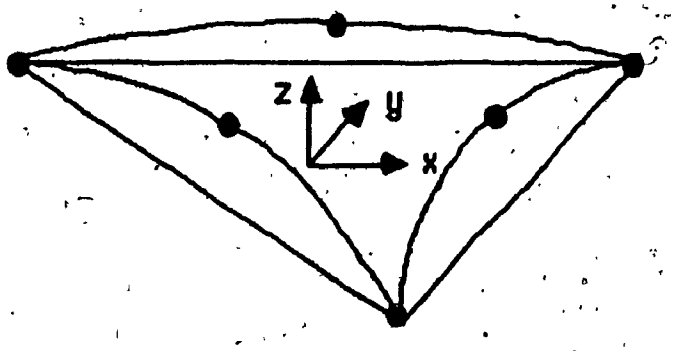

FIGURE 5.3: ZERO ENERGY MODE FOR T17-3

CHAPTER VI

DESCRIPTION OF NUMERICAL TESTS

6.1 Test Description

The availability of analytical solutions is a major constraint in the choice of test problems. On this basis, the performance of the hybrid elements under consideration was evaluated from the analysis of two rectangular sandwich plates, the first being simply supported and the second clamped. Both plates are subjected to a unit uniformly distributed load. The plates are assumed to lie in the xy plane (Fig.(6.1)) with the side parallel to X-axis (a) always being smaller than or equal to the side parallel to Y-axis (b).

For each case, the element convergence characteristics and the effect of varying the shear parameters and element aspect ratios or critical displacements and stress resultants were studied. The shear parameters for simply supported and clamped plates are defined by Eq. (6.1) and (6.2) respectively:

$$SP = S.a^2/D \qquad (6.1)$$

$$SP = S.a^2/(\pi^2.D) \qquad (6.2)$$

where S and D are defined by Eq.(2.5.3), (2.5.4), (2.9), (2.10) and (2.13). The aspect ratio is defined by Eq. (6.3):

$$AR = b/a \geq 1 \qquad (6.3)$$

Because of symmetry about both center lines, only a quarter of the plate was analyzed (Fig.(6.1)). Typical meshes for three types of elements are shown in Fig. (6.2). The boundary conditions for the model of the simply supported plate are given by Eq. (6.4).

$w = 0$ along both edges (6.4.1)

$\theta_x = 0$ along edge parallel to Y-axis and

along center line parallel to X-axis (6.4.2)

$\theta_y = 0$ along edge parallel to X-axis and

along center line parallel to Y-axis (6.4.3)

For the clamped plate, the boundary conditions are given by Eq. (6.5).

$w = 0$ along both edges (6.5.1)

$\theta_x = 0$ along both edges and

along center line parallel to X-axis (6.5.2)

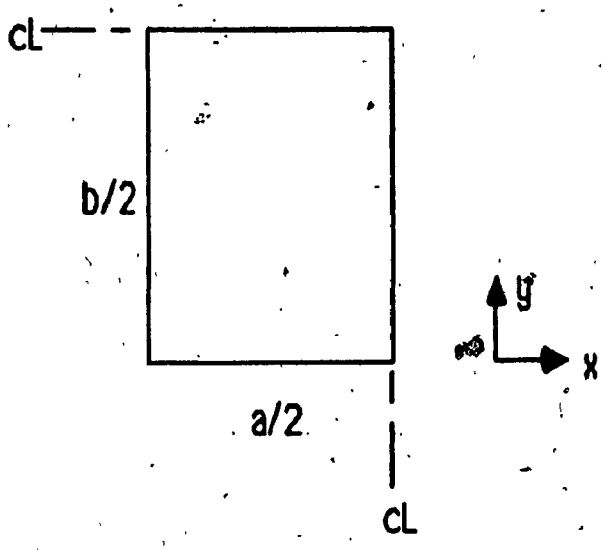

FIGURE 6.1: ORIENTATION OF THE QUARTER PLATE

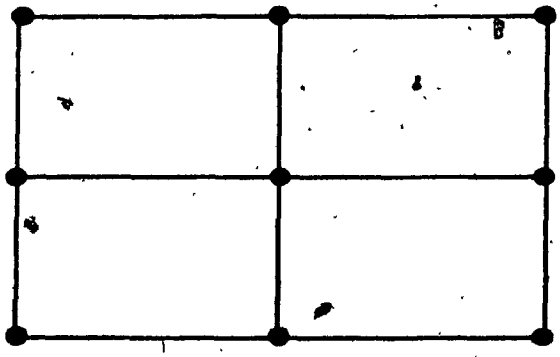

(a)

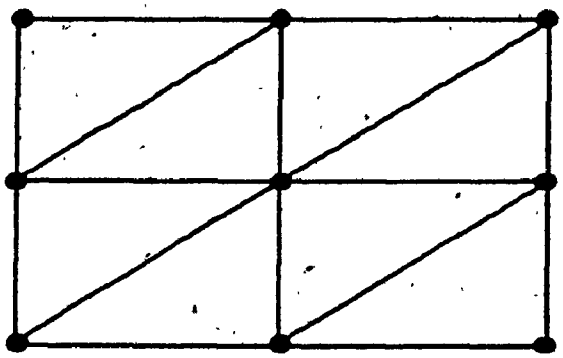

(b)

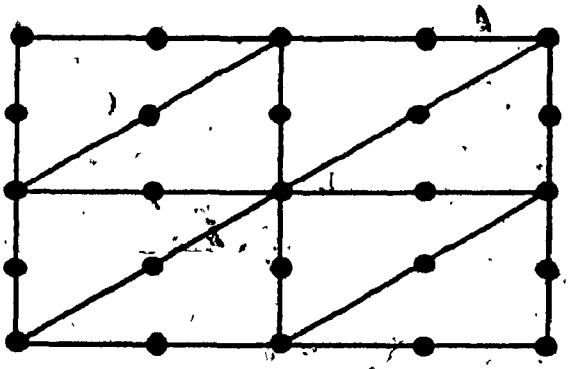

(c)

FIGURE 6.2: MESH ARRANGEMENT FOR (a) R5, R7, R11, R17; (b) T5, T7, T9 AND (c) T17-3 ELEMENTS

$\theta_y = 0$ along both edges and

along center line parallel to Y-axis (6.5.3)

The structure load vector was formed based on the tributary area rather than by the equivalent work principle. Even though the latter procedure is theoretically more consistent, both methods tend to yield the same results as the mesh is refined.

The convergence properties of the elements were tested on a simply supported plate with the geometric and material specifications given by Eq. (6.6) and (6.7) respectively.

$a = 3.048$ m (6.6.1)

$b = 6.096$ m (6.6.2)

$t = 6.350 \times 10^{-4}$ m (6.6.3)

$c = 5.017 \times 10^{-2}$ m (6.6.4)

$G = 5.196$ MPa (6.7.1)

$E = 68948.000$ MPa (6.7.2)

Thus, this plate has a shear parameter of 40 and an aspect ratio of 2. It is

noted that the ratio of d/t meets the requirement of Eq.(2.11) and E_c is assumed to be zero. This is consistent with assumptions 5 and 6 of Chapter I. The analytical solutions [29] for the maximum values of w, M_{xx} and M_{yy} are given in Table(6.1).

The convergence test for the clamped plate was performed using the following data:

$$a = 3.048 \text{ m} \tag{6.8.1}$$

$$b = 3.048 \text{ m} \tag{6.8.2}$$

$$t = 6.350 \times 10^{-4} \text{ m} \tag{6.8.3}$$

$$c = 5.017 \times 10^{-2} \text{ m} \tag{6.8.4}$$

$$G = 5.130 \text{ MPa} \tag{6.9.1}$$

$$E = 68948.000 \text{ MPa} \tag{6.9.2}$$

This plate has a shear parameter of 4 and an aspect ratio of 1. The analytical solutions for deflection at the center and normal moment at the mid-sides are given in the last two columns of Table (6.2). The values at these locations are maximum for the structure.

The shear parameter test was carried out with a mesh of 16

SP	w (m)	Mxx (N.m/m)	Myy (N.m/m)
10	0.206	6514	2972
20	0.152	6514	2972
40	0.124	6514	2972
80	0.111	6514	2972

TABLE 6.1: ANALYTICAL SOLUTIONS [29] FOR CONVERGENCE AND SHEAR PARAMETER TEST ON THE SIMPLY SUPPORTED PLATE

SP	w^{*} (m)	w (m)	M_{xx} (N.m/m)
0.0	∞	∞	2223
1.0	0.078	-	-
2.0	0.045	-	-
4.0	0.029	0.031	2626
8.0	0.021	-	-
16.0	0.016	-	-
∞	0.012	0.012	3286

TABLE 6.2: ANALYTICAL SOLUTIONS [29] FOR CONVERGENCE AND SHEAR PARAMETER TEST ON THE CLAMPED PLATE

rectangular or 32 triangular elements. The performance of the elements for different shear parameters was tested on a simply supported plate with the properties given by Eq. (6.6) and (6.7.2). For this test, the value of G was varied according to Eq. (6.1) to obtain different shear parameters. The analytical solution for deflections and moments for the range of shear parameters considered are given in Table (6.1). These solutions correspond to maximum values which occur at the center of the plate.

The shear parameter test for the clamped plate was performed on a plate specified by Eq. (6.8) and (6.9.2). G was changed according to Eq. (6.2) in order to yield different shear parameters. The analytical solutions for the maximum deflections, at the center of the plate, are given in the first column (w^*) of Table (6.2). In this case, the analytical solutions for stress resultants are not available.

The aspect ratio test was carried out using identical meshes to those of the shear parameter test. The accuracy of the elements for different aspect ratios was examined on a simply supported plate specified by Eq.(6.6.1), (6.6.3), (6.6.4) and (6.7). The value for b was varied in order to obtain different aspect ratios. The analytical solutions for maximum deflections and moments, at the center of the plate, for different aspect

ratios are given in Table (6.3).

A similar test for clamped plate was carried out using Eq.(6.8.1), (6.8.3), (6.8.4) and (6.9) as specifications. As before, b was changed in order to obtain different aspect ratios. In this case, analytical solutions were limited to maximum deflections which occurs at the center of the plate. These solutions are given in Table (6.4).

AR	w (m)	Mxx (N.m/m)	Myy (N.m/m)
1.0	0.057	3068	3068
1.2	0.075	4010	3209
1.4	0.091	4823	3241
1.6	0.105	5521	3158
1.8	0.116	6072	3068
2.0	0.124	6514	2972
3.0	0.147	7616	2588
4.0	0.153	7911	2460
5.0	0.154	7981	2402

TABLE 6.3: ANALYTICAL SOLUTIONS [29] FOR ASPECT RATIO TEST ON THE SIMPLY SUPPORTED PLATE

AR	w (m)
1.0	0.029
1.3	0.039
>1.4	0.049

TABLE 6.4: ANALYTICAL SOLUTIONS [29] FOR ASPECT RATIO TEST ON THE CLAMPED PLATE

CHAPTER VII

DISCUSSION OF THE RESULTS

The results for the convergence, shear parameter and aspect ratio tests will be considered in the following sections. Table (7.1) shows the list of symbols that are used for plotting the results for various hybrid elements. The figures for the results also include element T9-2 which was not described in Chapter V. The discussion of the performance of this element is excluded from the following sections. Details on this element are given in Chapter VIII.

7.1 Convergence Characteristics

The results for the convergence tests are presented in Fig.(7.1) to (7.5). Fig. (7.1) and (7.2) show the results for the maximum displacement at the center of simply supported and clamped plates. It is noted that all elements with the exception of T17-3 converge to the analytical value as the mesh is refined. T17-3 seems to converge to a value less than the analytical solution. Results for T5, T7 and T9 approach the analytical value

LIST OF SYMBOLS FOR HYBRID ELEMENTS

ELEMENT	REFERENCE	SYMBOL
R5	[15]	●
R7	[15]	■
R9	[15]	▼
R11	[15]	⧋
R17	[11]	◇
T5	[8]	○
T7	[8]	□
T9	[8]	▽
T17-3	[6]	◊
T9-2		○-

Table 7.1: List of Symbols

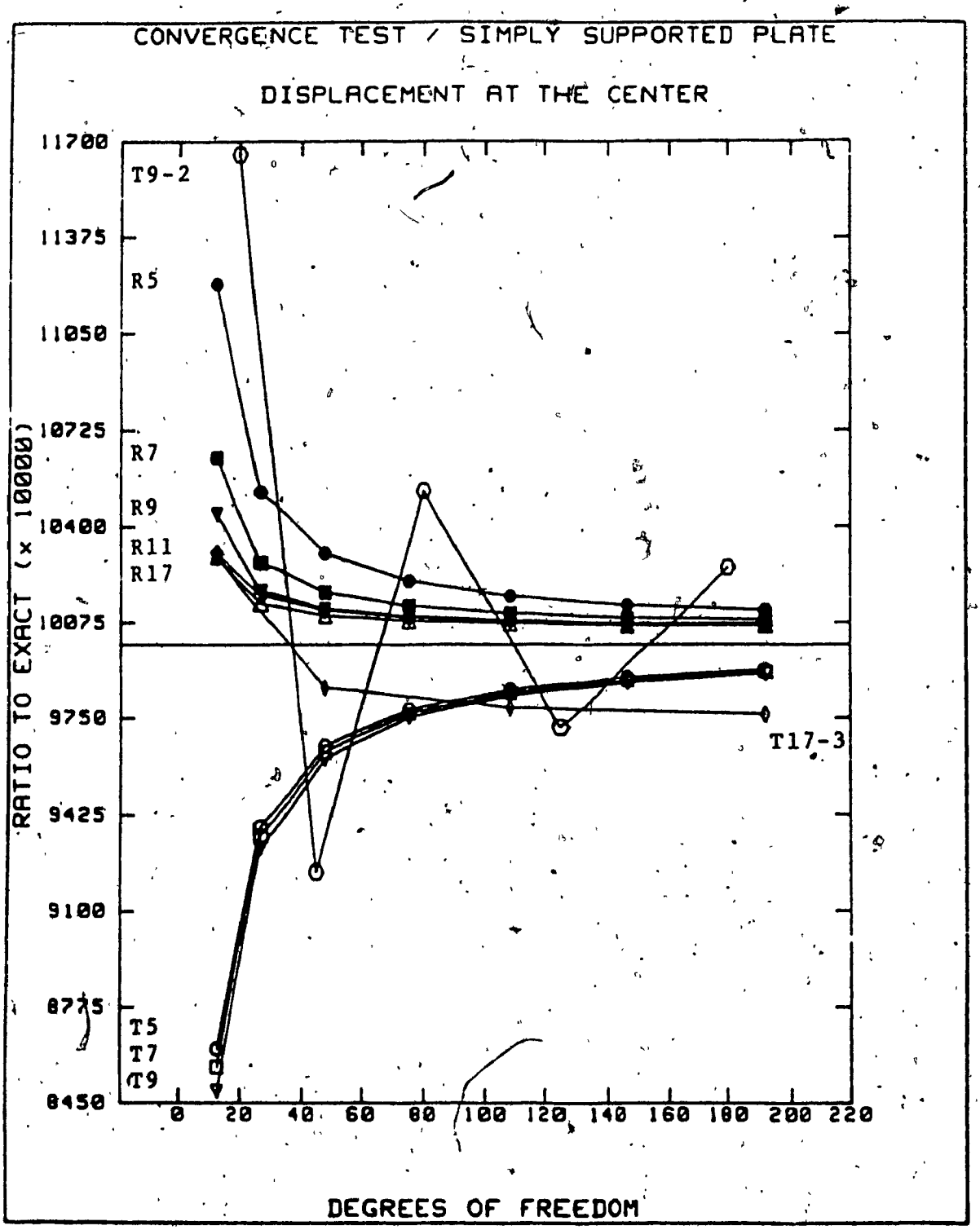

Figure 7.1: Convergence Test - w at the Center of Simply Supported Plate

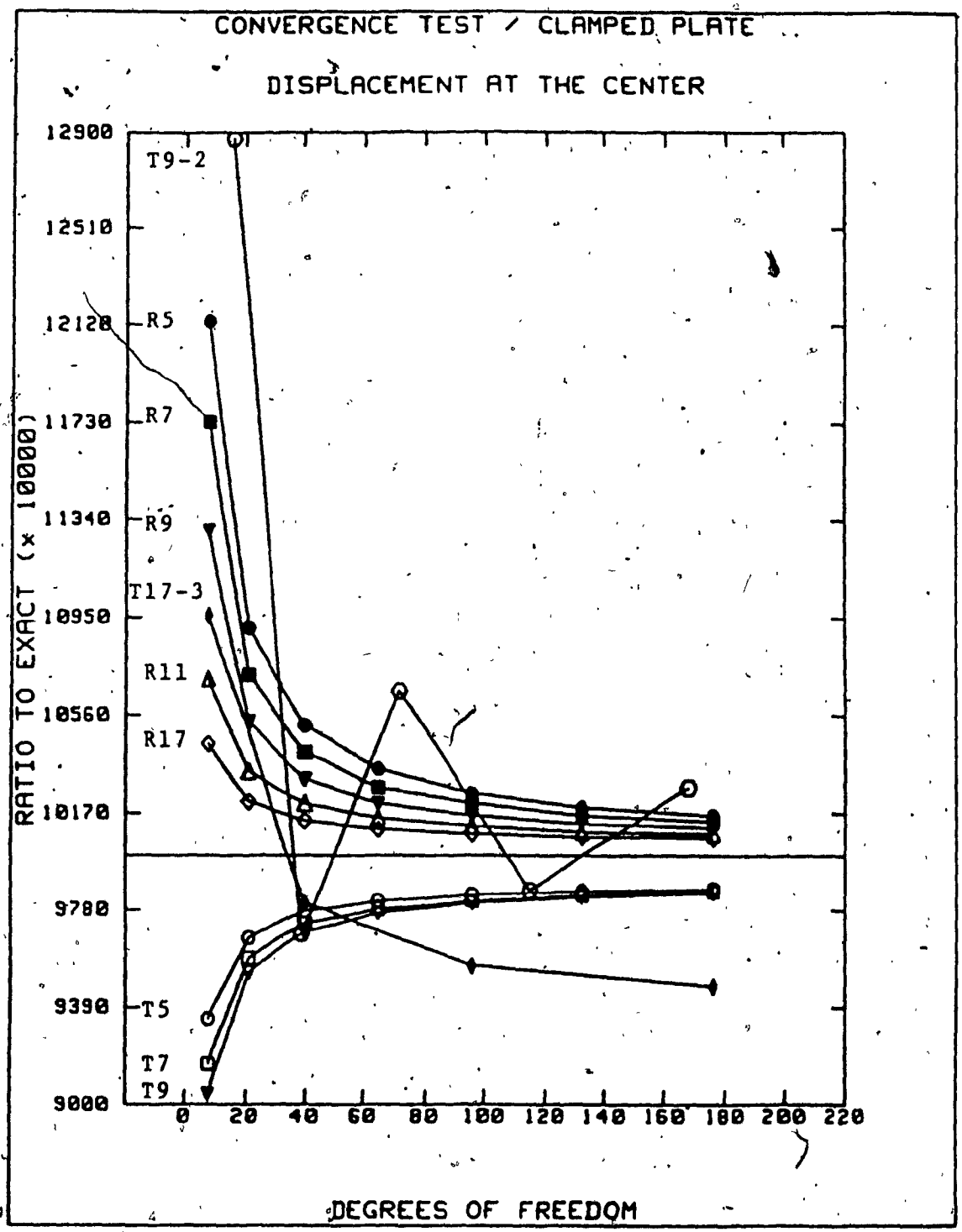

Figure 7.2: Convergence Test - w at the Center of Clamped Plate

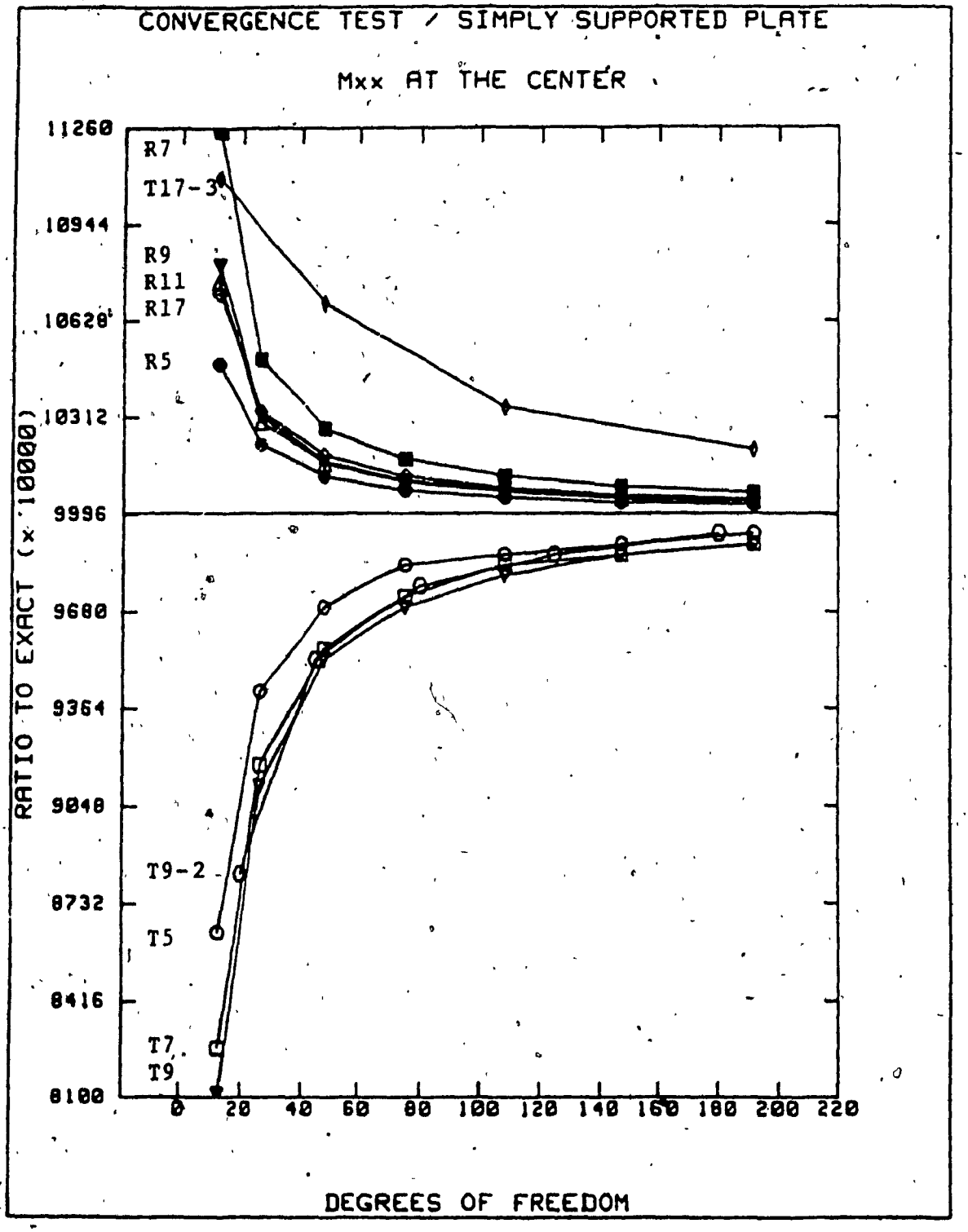

Figure 7.3: Convergence Test - M_{xx} at the Center of Simply Supported Plate

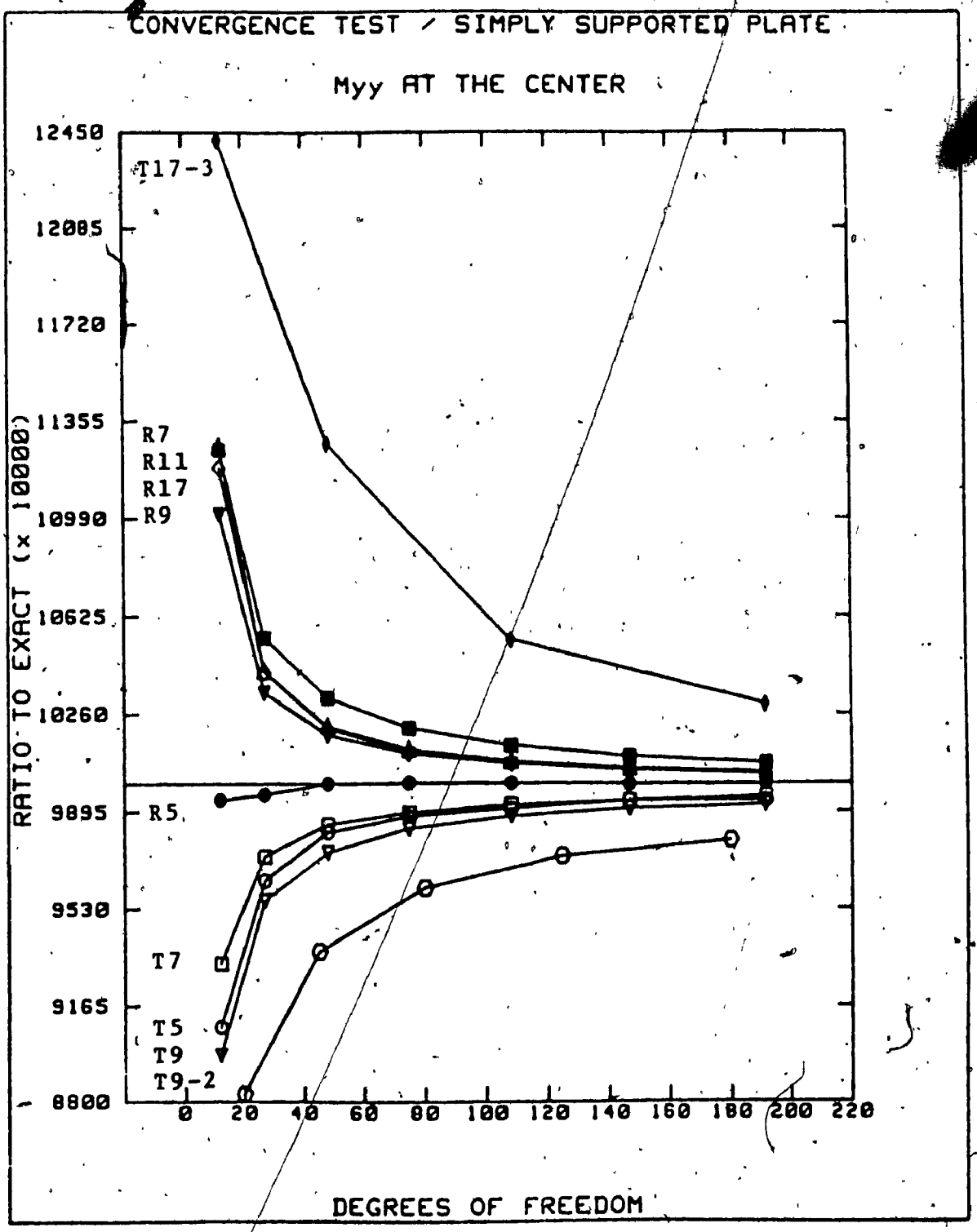

Figure 7.4: Convergence Test - M_{yy} at the Center of Simply Supported Plate

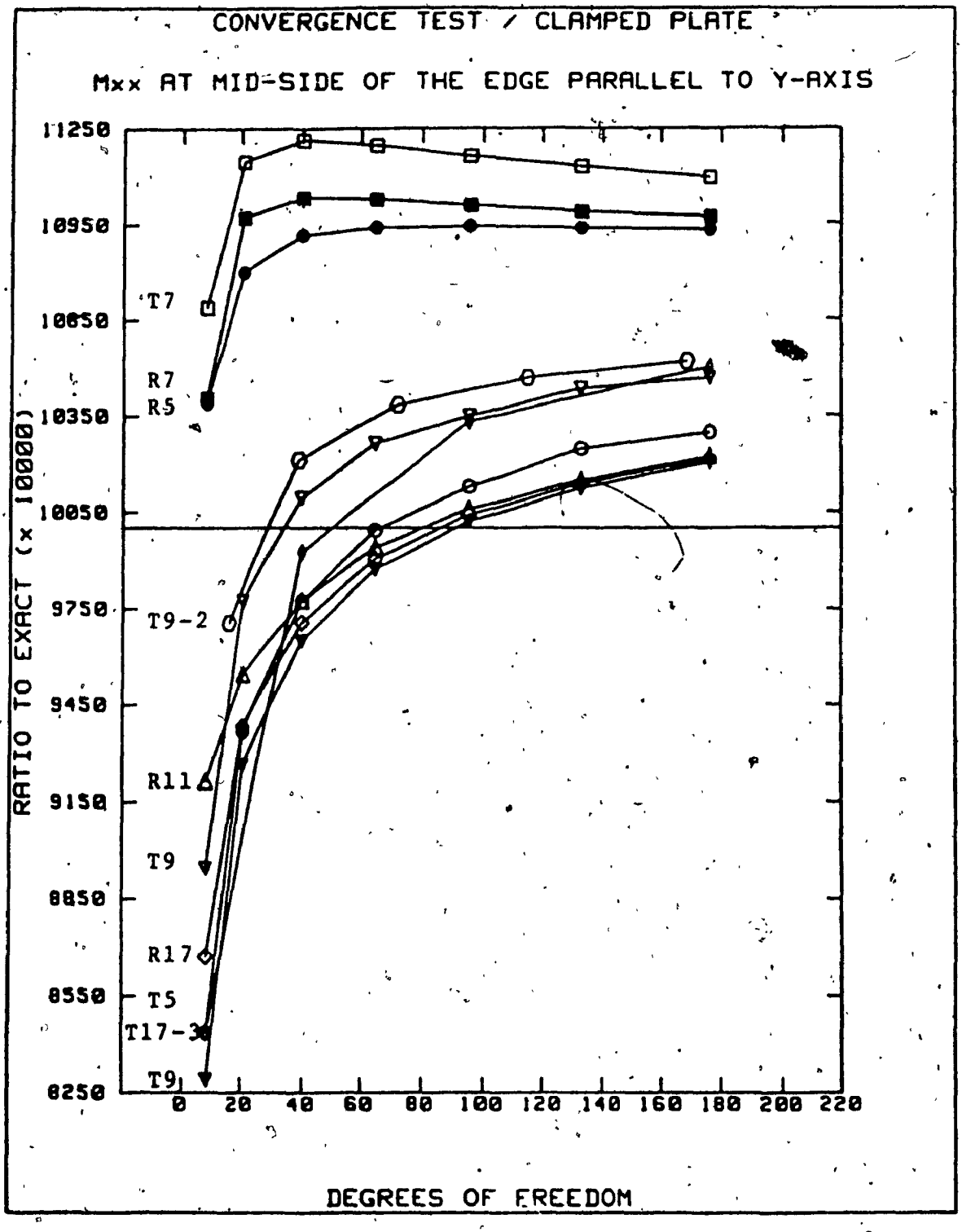

Figure 7.5: Convergence Test - Normal Moment at Mid-side of Clamped Plate

from below. Element T9 is stiffer than T7 which in turn stiffer than T5.

Results for elements R5, R7, R9, R11 and R17 approach the analytical solution from above. That is these elements tend to be too flexible. For all mesh sizes, the deflection results from the elements R5, R7, R9 and R11 show that these elements exhibit a lesser degree of flexibility in the same sequence. In other words, for all mesh sizes, R11 is stiffer than R9 which is stiffer than R7 and so on. The results for R11 and R17 are the same for the simply supported plate. For the clamped plate, R17 is stiffer than R11. From the hierarchy of the above results, it can be concluded that for the family of rectangular and triangular elements under consideration (T17-3 excluded), addition of extra stress parameters makes an element stiffer.

The results for M_{xx} and M_{yy} at the center of the simply supported plate are shown in Fig. (7.3) and (7.4) respectively. The results for all elements converge towards the analytical solution as the mesh is refined. Results for T5, T7 and T9 are less than the analytical value whereas R7, R9, R11 and R17 yield results that are larger (Table (6.1)). The results within each of the above groups is less than 1% apart for a mesh of about 100 degrees of freedom.

For the element R5, M_{xx} approaches the analytical solution from above whereas M_{yy} approaches it from below. This can be explained by noting that for R5, the assumed functions for M_{xx} and M_{yy} are not symmetrical in x and y (Eq.(5.7)). Therefore, it is expected that the accuracy obtained is dependent on the axes orientation. T5 has the same stress distribution as R5. However, the test results for T5, for moments at the center, are the average values from the two elements which share the center node (Fig.(6.2b)). The averaging process has yielded results that seem consistent. Nevertheless, elements R5 and T5 should be used with caution because they both lack invariance towards the choice of the axis system. Finally, it is noted that results for T17-3 converge towards the analytical solutions from above but not as rapidly as the other elements.

The results for the normal moment at the mid-side of the clamped plate is shown in Fig. (7.5). The results for all elements seem to converge to a value larger than the analytical solution (Table (6.2)). This can be explained noting that the boundary conditions used in the analytical solution are those given by Eq.(2.8.3) in addition to the third condition:

$$M_{xy} = 0 \qquad \text{(for y=constant)} \qquad (7.1)$$

Analytical solution for the more practical boundary condition:

$$\gamma_x' = 0 \qquad \text{(for y=constant)} \qquad (7.2)$$

is not available. These boundary conditions differ from those used in the finite element model as given by Eq. (6.5). Furthermore, the discrepancy between boundary conditions affects the results most adversely near the boundaries. This is evident noting that the results for moment at the center of the simply supported plate are in general more accurate than those at the mid-side of the clamped plate even though a similar discrepancy between the boundary conditions (Eq.(2.8.2) and (6.4)) existed for the former case as well.

From the results for the convergence test, it can be concluded that the elements T5, T7, T9, R5, R7, R9, R11 and R17 converge towards the analytical solutions for the simply supported case and for deflection at the center of the clamped plate. These elements tend to become stiffer as the number of independent stress parameters is increased. Element T17-3 does not perform as well as the other elements especially for the simply supported plate.

It is important to note that the accuracy of the results for the simply supported plate is generally of the same order for displacements

and stresses. This is because the stresses for hybrid elements, unlike displacement elements, are not calculated from derivatives of the displacements. Finally, the stress results near the boundaries must be interpreted cautiously. Deviations from the analytical solutions are likely to be accentuated at these locations when bounadry conditions in the analytical solution differ from those in the finite element model.

7.2 Influence of Shear Parameter on Accuracy

Results for the shear parameter test are presented in Fig. (7.6) to (7.9). It should be repeated that shear parameters for simply supported and clamped plates are defined differently as indicated by Eq.(6.1) and (6.2). Ideally, the accuracy of an element should not be affected by the variations in the shear parmeter. In the above figures, where the ratio to the analytical (exact) is plotted on the vertical axis, this ideal behavior would correspond to a horizontal line.

The analytical solutions for displacements decrease with an increasing shear parameter as shown in Tables (6.1) and (6.2). Also, the moments for the simply supported plate are independent of the shear parameter. The analytical solution for the moment at the mid-side of the

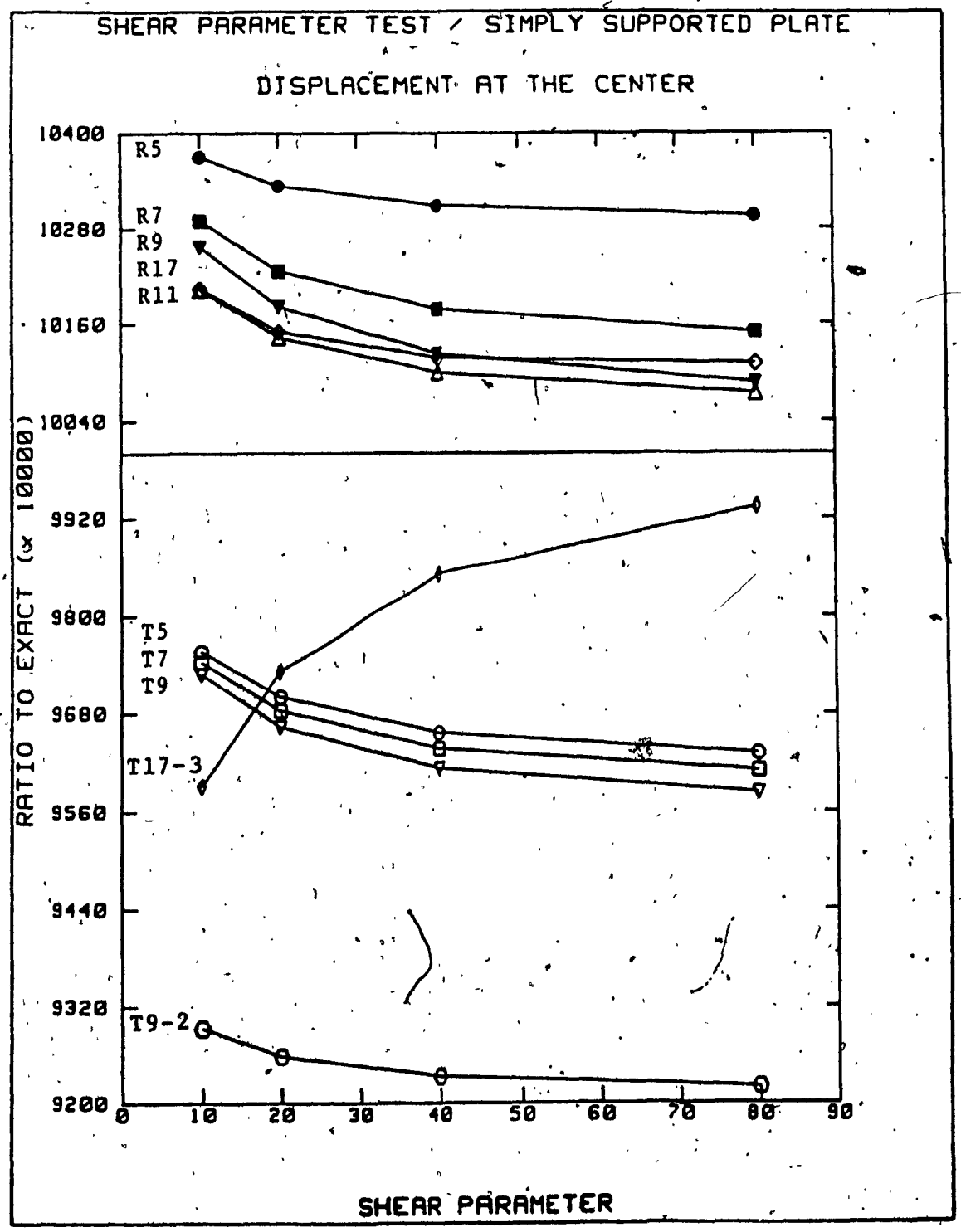

Figure 7.6: Shear Parameter Test - w at the Center of Simply Supported Plate

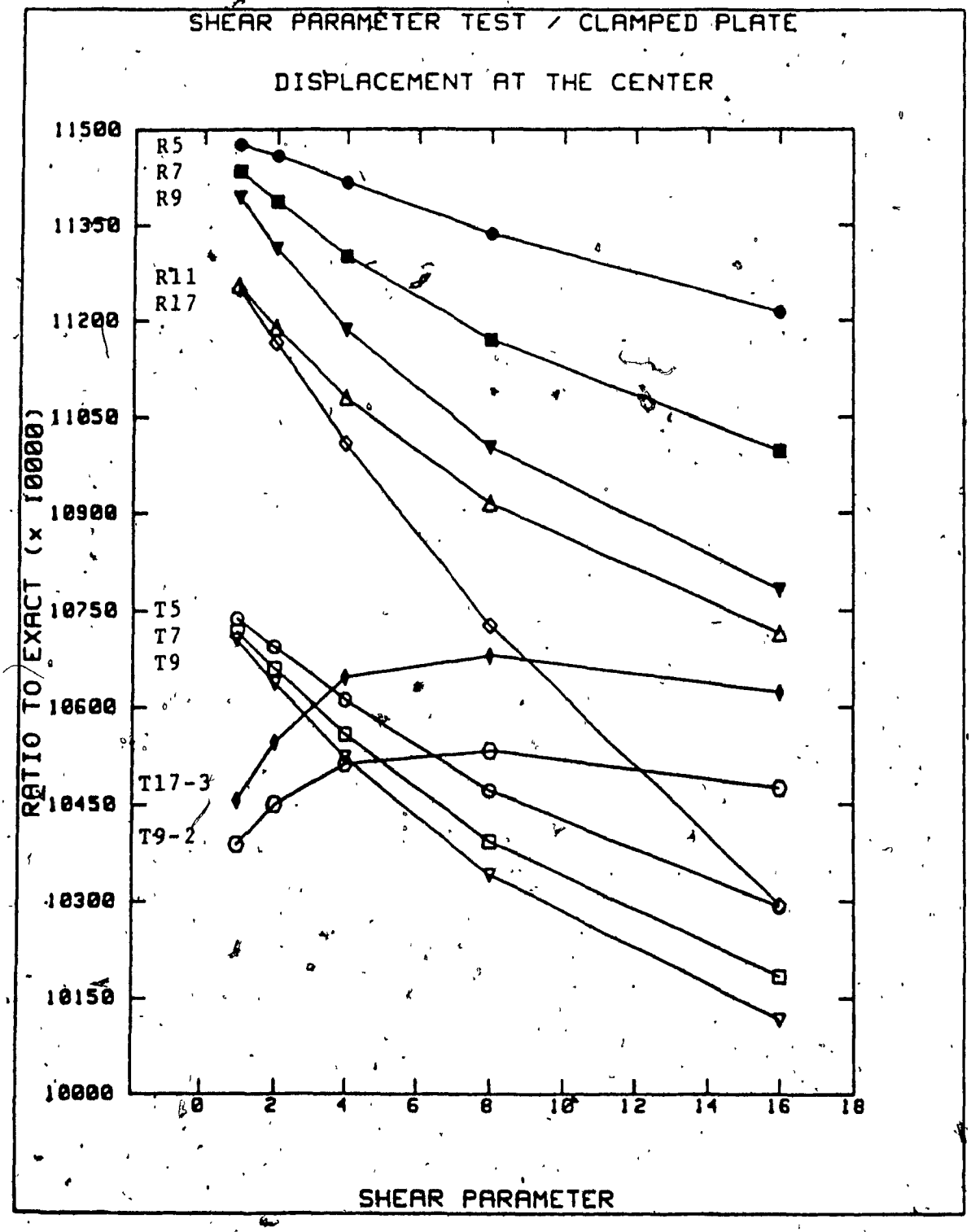

Figure 7.7: Shear Parameter Test -- w at the Center of Clamped Plate.

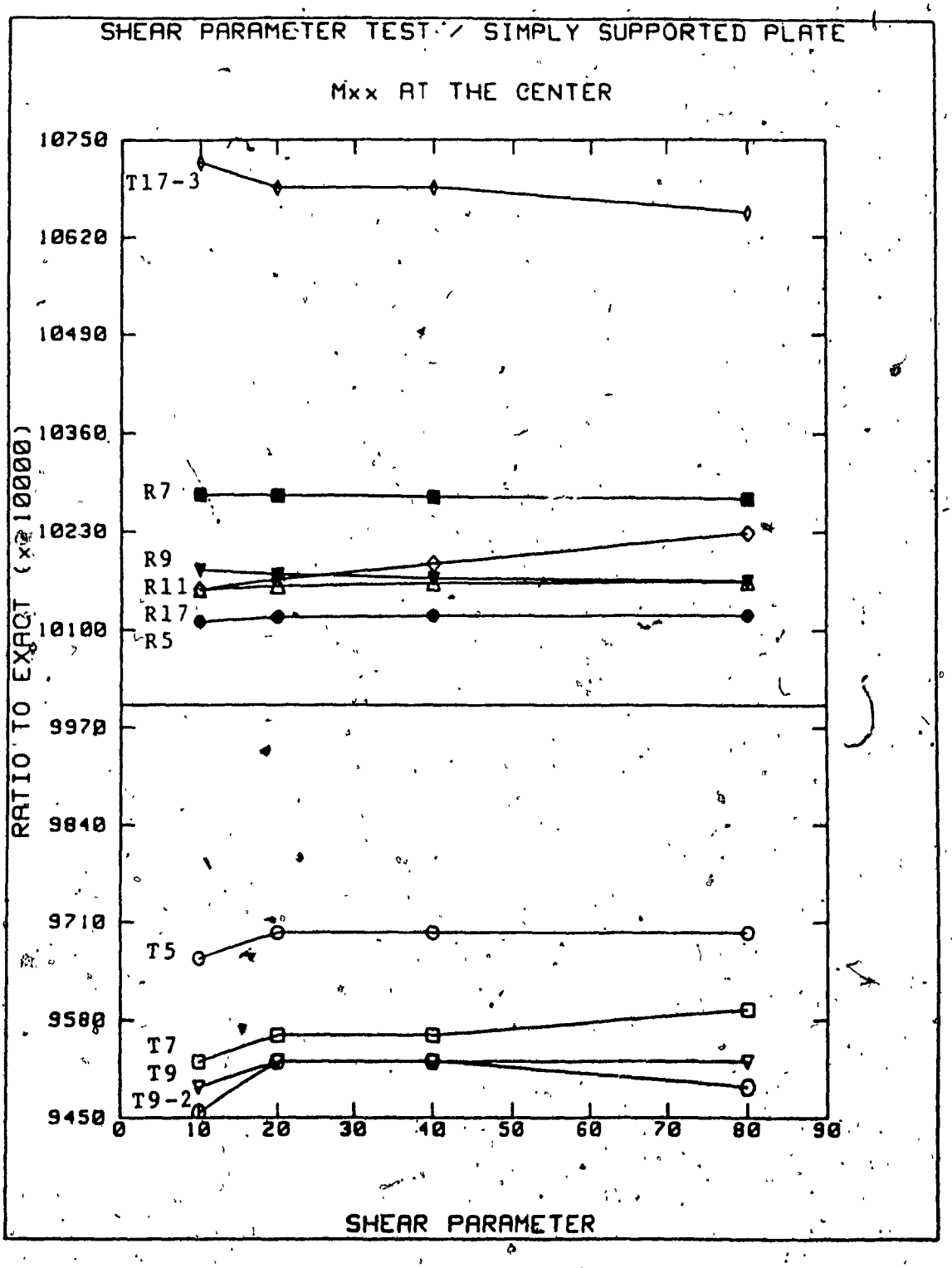

Figure 7.8: Shear Parameter Test - M_{xx} at the Center of Simply Supported Plate

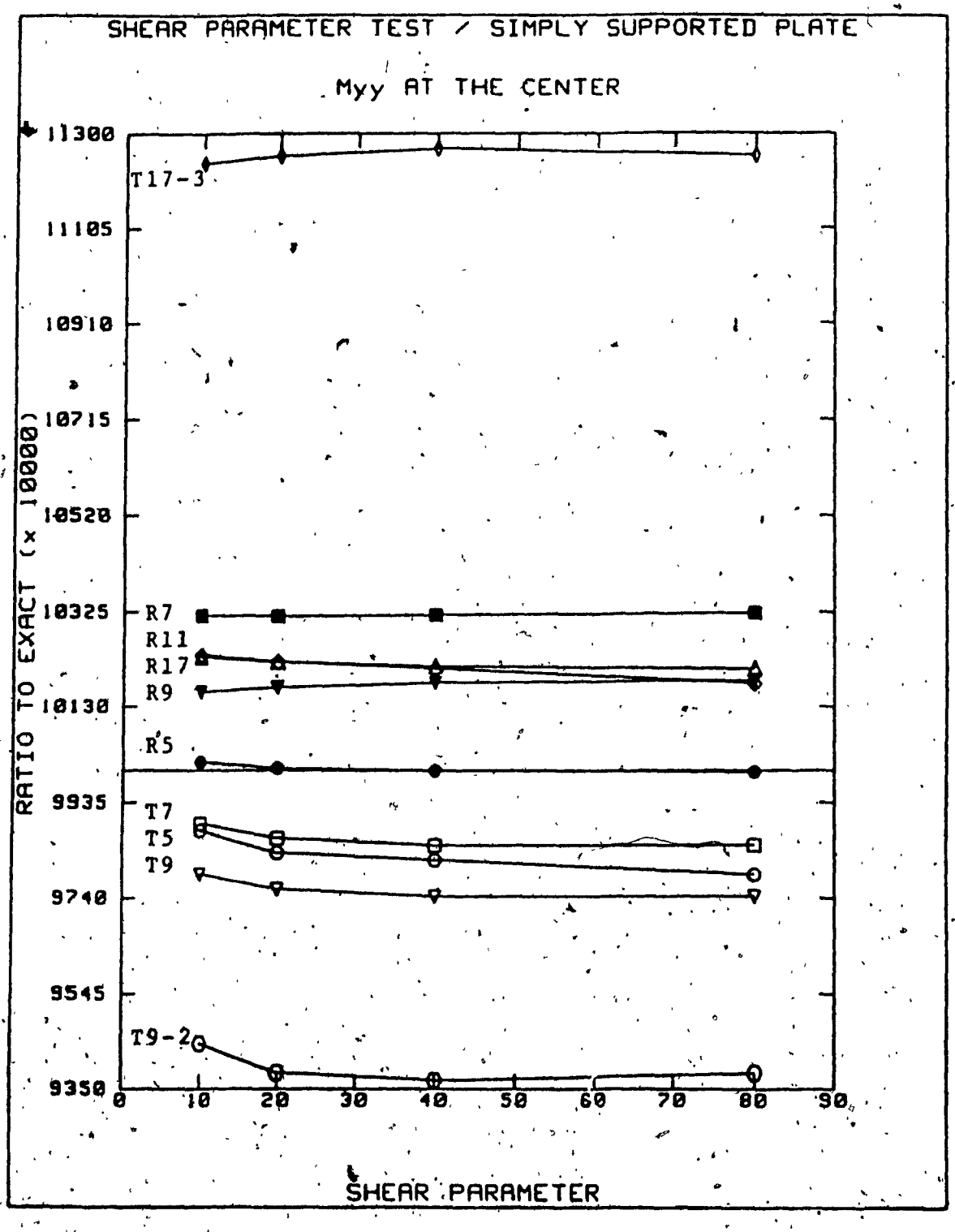

Figure 7.9: Shear Parameter Test - M_{yy} at the Center of Simply Supported Plate

clamped plate is not available for the range of shear parameters considered. However, for a plate with no transverse shear deformation, this moment is given in Table (6.2). It is known that the transverse shear deformations have a relieving effect on the magnitude of this moment.

The results for displacement at the center of the simply supported plate is shown in Fig. (7.6). In this case, all elements, with the exception of T17-3 perform satisfactorily. Element T17-3 seems to perform more accurately for higher shear parameters where the contribution of transverse shear deformations is less significant. It is noted that the relationship between the displacement results and the number of β's, which was observed in the last section, is maintained here. That is, for the shear parameters considered, displacement results for a family of elements seem to become stiffer with increasing number of β's. This is evident from the results for T5, T7 and T9 group as well as R5, R7, R9 and R11 group. Element R17 deviates slightly from this pattern. The largest deviation occurs when the shear parameter is 80. At this point, ratio to exact for R17 is 0.6% larger than R11 instead of being smaller. This could be due to the fact that the tests for R17 were carried out using a separate set of programs. The differences in coding of these programs might have caused

some numerical discrepancies in the results.

Results for the displacement at the center of the clamped plate are shown in Fig.(7.7). Once more, the relationship between displacement results and the number of β's is confirmed for two groups of T5, T7 and T9 as well as R5, R7, R9, R11 and R17. The above elements seem to be more accurate for larger shear parameters. this can be explained noting that the analytical solution (Table (6.2)) underestimates the displacements for lower values of the shear parameter [29]. This is due to the particular choice of displacement functions in the analytical solution. Consequently, the ratios to exact for the lower shear parameters are overstated in Fig.(7.7). Element T17-3 behaves differently from other elements. The maximum variation of the ratio to exact for this element is only 2% which is much less than the corresponding value for the other elements.

The results for moments (Fig.(7.8) and (7.9)) at the center of simply supported plate show a maximum variation of 2% for the ratios to exact over the range of shear parameters considered. This is expected because the moments for the simply supported plate are independent of the shear parameter as shown in Table (6.1).

Due to the unavailability of analytical solutions, the results for the

moment at the mid-side of the clamped plate are not plotted. However, the raw test results indicate that all elements yield larger moments for increasing shear parameters as expected by theory.

7.3 Influence of Aspect Ratio on Accuracy

The results for the aspect ratio tests are shown in Fig. (7.10) to (7.13). Fig. (7.10) shows the displacement at the center of the simply supported plate. It can be seen that the accuracy of elements T5, T7 and T9 as compared to analytical solutions of Table (6.3) is not significantly affected by the changes in aspect ratio. Accuracy of elements R5, R7, R9, R11 and R17 is slightly influenced by the variations in aspect ratio. For these elements, the results are generally more accurate for higher aspect ratios. It is noted that the sensitivity of these elements to aspect ratio decreases with increasing number of β's. That is element R11 is less sensitive to changes in aspect ratio than R9 and so on. Also, once more, for two groups of T5, T7, T9 and R5, R7, R9, R11 displacement results at any aspect ratio, tend to be stiffer for the element with the larger number of β's. Element R17 does not fit in this pattern for the reasons mentioned earlier.

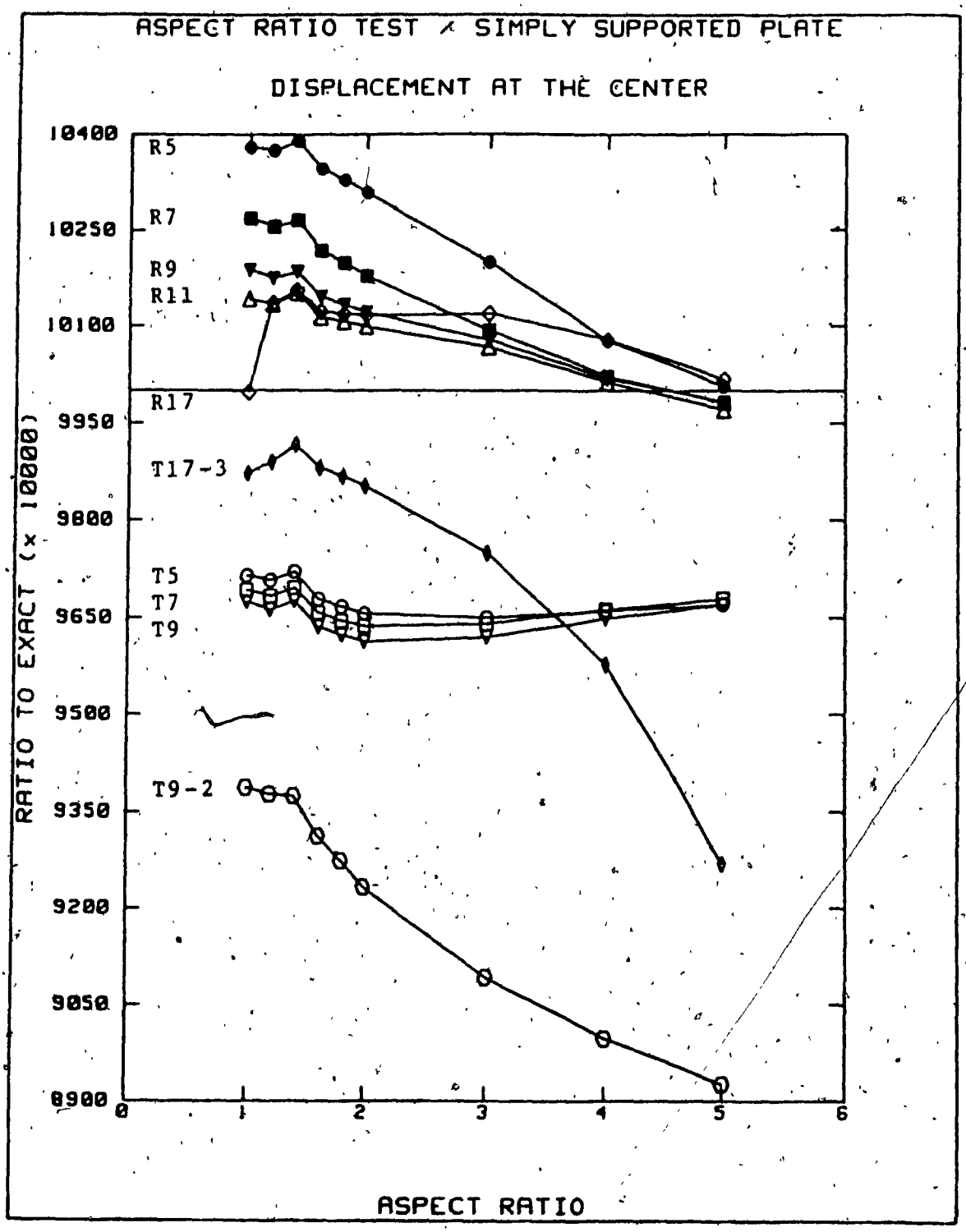

Figure 7.10: Aspect Ratio Test - w at the Center of Simply Supported Plate.

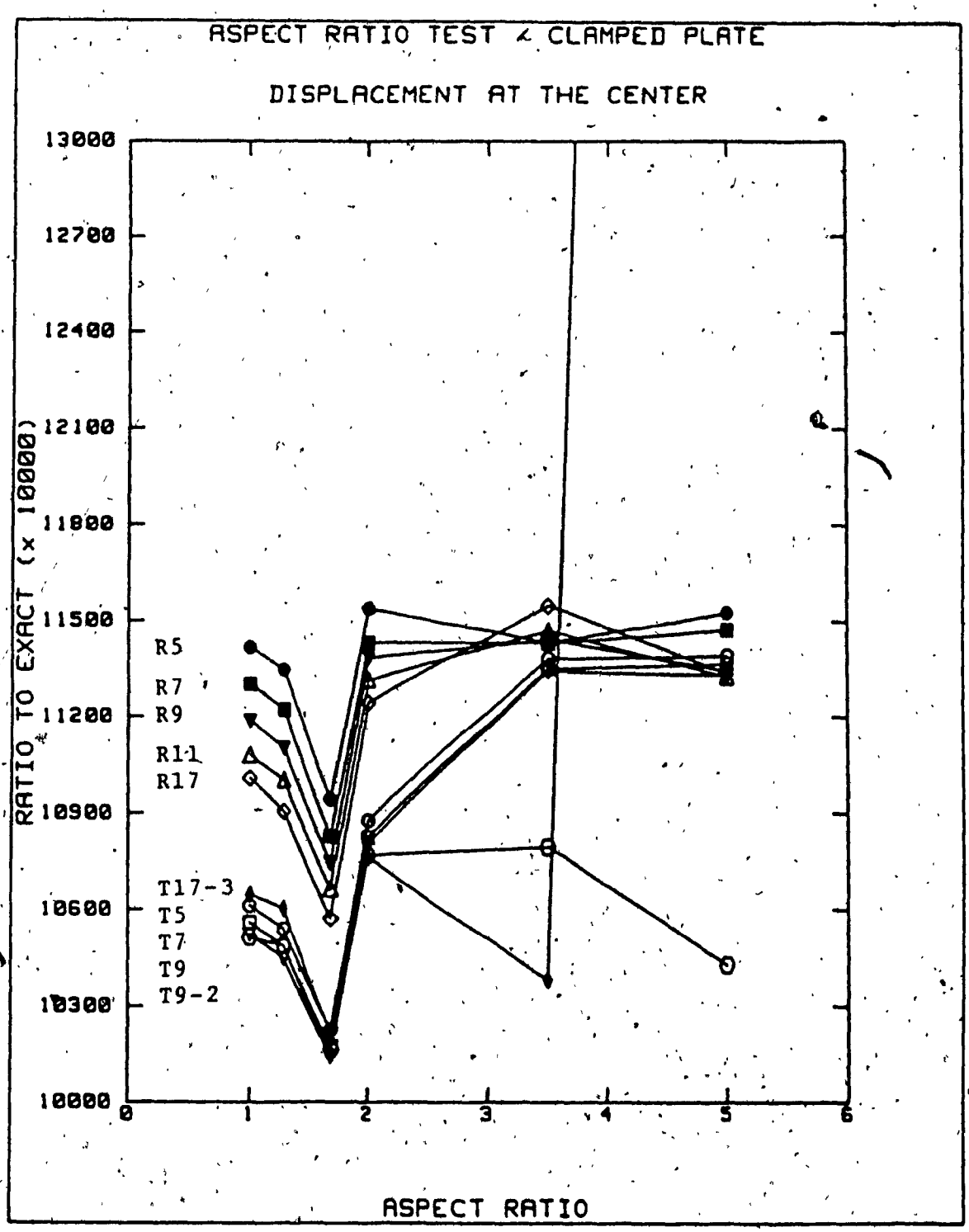

Figure 7.11: - Aspect Ratio Test - w at the Center of Clamped Plate

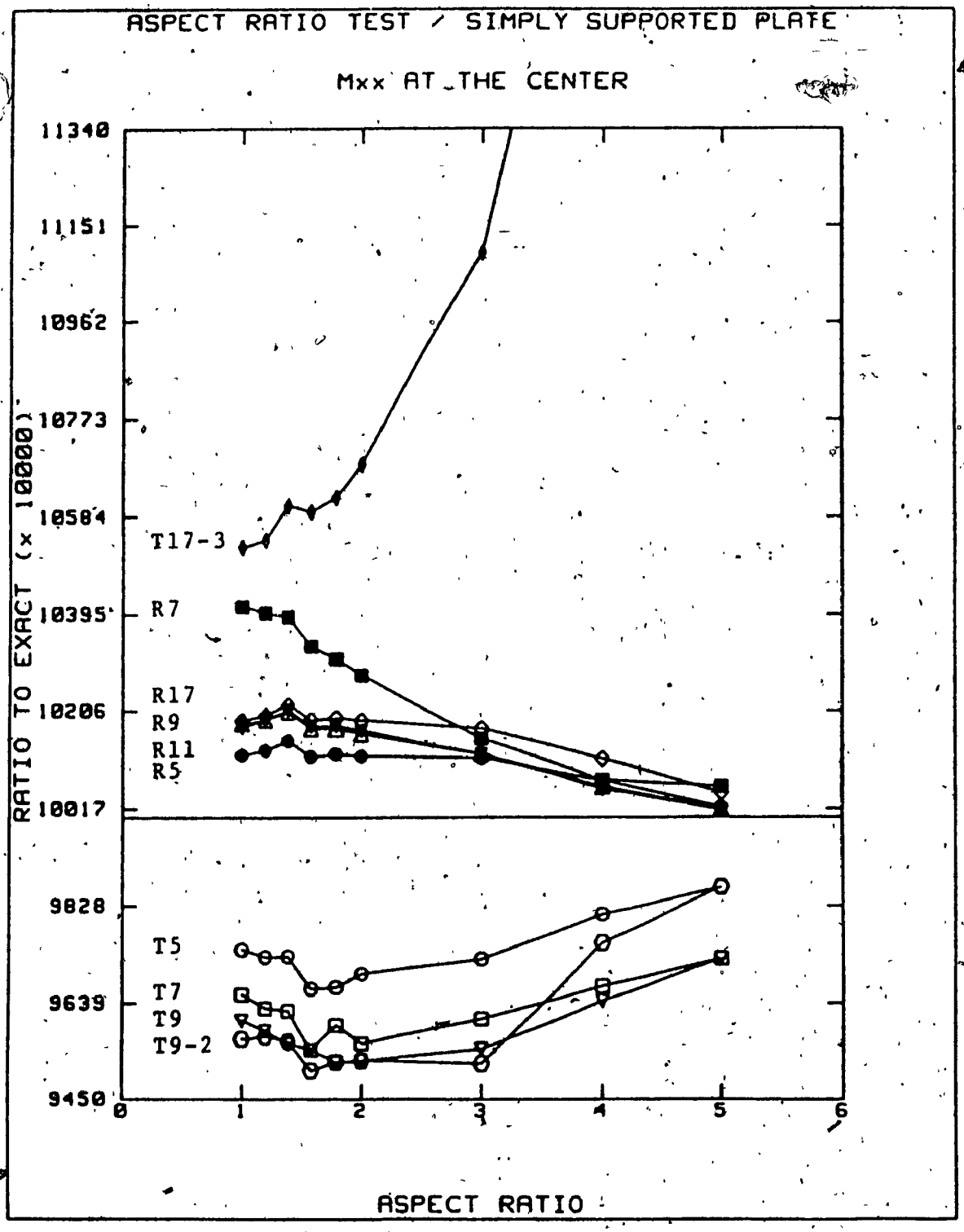

Figure 7.12: Aspect Ratio Test - M_{xx} at the Center of Simply Supported Plate

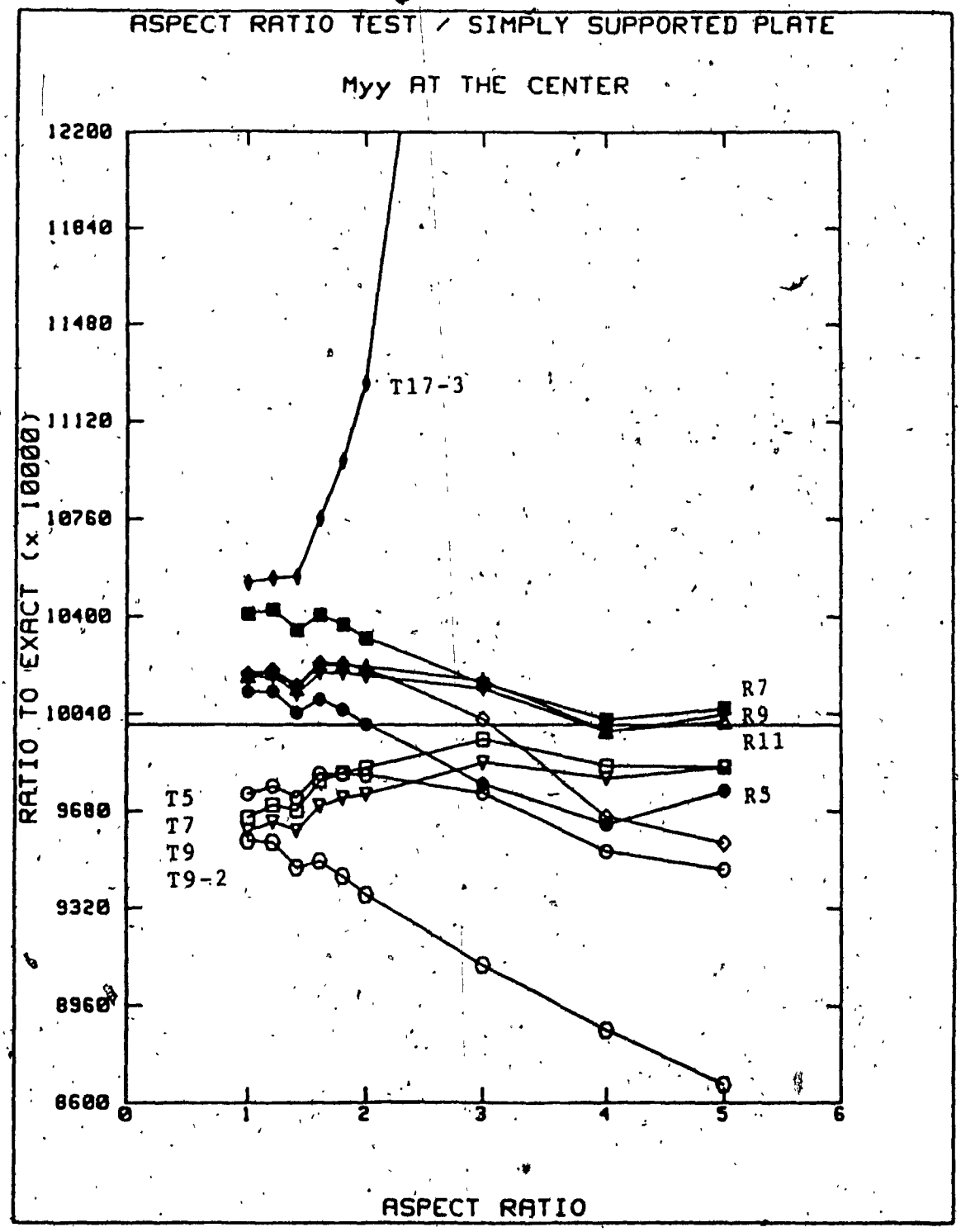

Figure 7.13: Aspect Ratio Test - M_{yy} at the Center of Simply Supported Plate

Element T17-3 performs satisfactorily for aspect ratios of less than 2 and after that the accuracy for the displacement results deteriorates rapidly. This is due to the existence of a zero energy mode (Fig. (5.3)) in this element. The results for elements R5, R7 and R9 are not affected by their zero energy modes (Fig. (5.2)) because zero energy modes are triggered under specific loading conditions. For example, the zero energy mode of Fig. (5.2b) causes anticlastic bending in an element which does not exist in a simply supported plate subjected to a uniformly distributed load. However, it has been shown [28] that for problems with anticlastic bending, this zero energy mode could distort the results.

Fig. (7.11) shows the displacement results at the center of the clamped plate. In this figure, a discontinuity in slope of all curves exist at an aspect ratio of 1.7. This can be explained noting that in the analytical solutions (Table (6.4)), a different displacement function has been used for aspect ratios larger than 1.4 [29].

As previously described, for a given aspect ratio, the displacement results in each of the two groups of T5, T7, T9 and R5, R7, R9, R11 and R17 show that the elements tend to become stiffer with increasing number of β's. Also, results for these elements seem to be equally sensitive to

changes in aspect ratio. These patterns are distorted for aspect ratios greater than 2. Element T17-3 yields results that are in line with the other elements for aspect ratios less than 2. For larger aspect ratios, the accuracy of the results deteriorates rapidly.

Fig. (7.12) shows the results for M_{xx} at the center of the simply supported plate. The analytical solution for M_{xx} increases with aspect ratio as shown in Table (6.3). Elements T5, T7, T9, R5, R7, R9, R11 and R17 perform quite well for the range of aspect ratios considered. The maximum variation in accuracy is about 3.5% and belongs to R7. For this element, the accuracy remains stable for aspect ratios of less than 2 and afterwards, the accuracy improves. The accuracy of results for T17-3 become unacceptable for large aspect ratios. For instance, at an aspect ratio of 4, the error is about +21%.

Fig. (7.13) represents the results for M_{yy} at the center of the simply supported plate. The analytical solution for M_{yy} decreases with increasing aspect ratios as shown in Table (6.3). Elements T7 and T9 perform satisfactorily whereas the accuracy of T5 seems to diminish for aspect ratios larger than 1.6. The superiority of T7 and T9 in this set of results is

due to larger number of β's in their stress fields. The accuracy of R7, R9 and R11 improves for higher aspect ratios. Elements R5 and R17 overestimate M_{yy} for low aspect ratios and underestimate it for higher ratios, that is the curve for these elements crosses the exact line. Element T17-3 yields unacceptable results for aspect ratios higher than 1.4. For instance, at an aspect ratio of 3, this element yields an error of +46% in M_{yy}.

The results for normal moments at the mid-side of the clamped plate are not plotted due to the unavailability of analytical solutions.

7.4 Summary of Results

From the above results, it can be concluded that results obtained from assumed stress hybrid elements may approach the analytical value from above or below. Therefore, their results are not bounded. It is evident from the results that for a family of elements, increasing the number of independent stress parameters makes the elements stiffer.

From a comparison of the accuracy for moments between the two types of plates in the convergencetest, it can be concluded that the results

are very sensitive to the choice of boundary conditions. Therefore, the analytical results, specially near the boundaries, are not a very good measure of evaluating the performance of an element unless identical boundary conditions are used in both the analytical solution and the finite element model. Nevertheless, the analytical solutions remain the best benchmark in numerical tests.

All the above hybrid elements perform quite well for a wide range of shear parameters. In the aspect ratio test, for the element with larger number of independent stress parameters in a given family, the accuracy of displacement results was generally less sensitive to variations in aspect ratio.

Overall, element T17-3 performs poorly for aspect ratios greater than 1.4. This is due to the existence of its unsuppressed zero energy mode (Fig. (5.3)). Therefore, it is recommended that no element having zero energy modes, capable of occuring in a mesh, be used for finite element modelling. These modes may cause severe inaccuracies in the results under certain loading conditions.

Element T9 performs consistently well in all tests. It has one zero energy mode that does not occur in a mesh. Its advantage over T5 is that

its performance is less sensitive to changes in aspect ratio. Also, its stress functions are invariant with respect to the choice of the coordinate system. Element T7 also performs quite well but it has the shortcoming of having a constant M_{xy} distribution. Therefore, the use of T9 is recommended where triangular elements are required eg. for modelling of plates with complex geometry.

Rectangular elements are computationally simpler to formulate than triangular elements. Among the elements in this group, elements R5, R7 and R9 each have at least one potentially troublesome zero energy mode (Fig. (5.2b)) and therefore, their use should be avoided. Elements R11 and R17 perform consistently well. The results for these two elements is in close agreement in all cases. Therefore, the use of R11 is recommended because it requires less computation time than R17.

CHAPTER VIII

AN EXPERIMENTAL ELEMENT

8.1.- Element Description

In the previous chapter, it was concluded that elements T9 and R11 perform satisfactorily for all the numerical tests considered. In this chapter, an alternative element is considered and its performance is evaluated.

The shape of this element is chosen to be triangular because triangles provide more versatility in modelling a plate of arbitrary shape. Another alternative would have been a general quadrilateral element. However, closed form solutions for surface integrals for general quadrilaterals do not exist and numerical integration could considerably increase the computation time involved.

The stress distribution for this element is given by Eq. (5.9). This choice was made because it proved satisfactorily for T9. Also, with lesser number of stress parameters, the shortcomings associated with T5 and T7 would surface.

In choosing boundary displacements, the order of θ cannot be less than the order of the first derivative of w (Eq.(4.6)). For R11, w and θ are linear (Eq.(5.4)). Therefore, γ must be linear. For T9, w is given by Eq.(5.10). Therefore, the first derivative of w is linear. Since θ is also linear (Eq.(5.4.2) and (5.4.3)), then γ could be linear or constant. The displacement field for R11 is the simplest possible for an assumed stress hybrid plate bending element. However, this distribution has shown to be unsuitable for triangular plate bending elements [9,11]. Therefore, as an alternative, quadratic w was chosen along the edges (Eq.(5.6.1)) while θ was kept linear (Eq.(5.4.2) and (5.4.3)). In order to accomodate quadratic variation of w, mid-side nodes were introduced with only deflection as a degree of freedom. Thus the element has 6 nodes and 12 degrees of freedom.

The results of preliminary tests for this element showed that it was too flexible. This is due to the existence of three zero energy modes. For thin plate hybrid elements, it has been shown [27] that the elements stiffen as the order of the edge displacement shape functions is reduced. On this basis, the displacement function along only one of the edges was reduced to first order and the corresponding mid-side node was removed. The result

was element T9-2 with 5 nodes and 11 degrees of freedom. This element has also three zero energy modes as shown in Fig.(5.1) and (8.1). This element was subjected to the same set of numerical tests as the other elements. A typical mesh arrangement for this element is shown in Fig.(8.2). The test results for T9-2 are shown in Fig. (7.1) to (7.13). The discussion of these results is pursued in the next section.

8.2 Test Results

In the convergence test, the displacement results for T9-2 oscillate about the analytical solution (Fig.(7.1) and (7.2)). The results are more accurate for finer meshes. The stiffer displacement results correspond to meshes with an odd number of elements. The oscillation of the results is due to the sensitivity of the element to mesh arrangement. This sensitivity arises from an unequal number of nodes along the edges. The results for the moments of the simply supported and clamped plates are in line with other elements (Fig. (7.3) to (7.5)).

The accuracy of results for the displacement and moment for the simply supported plate is insensitive to changes in the shear parameter (Fig.(7.6), (7.8) and (7.9)). The results for the displacement at the center

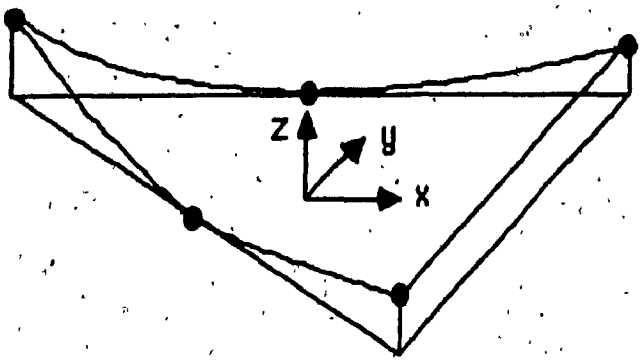

(a)

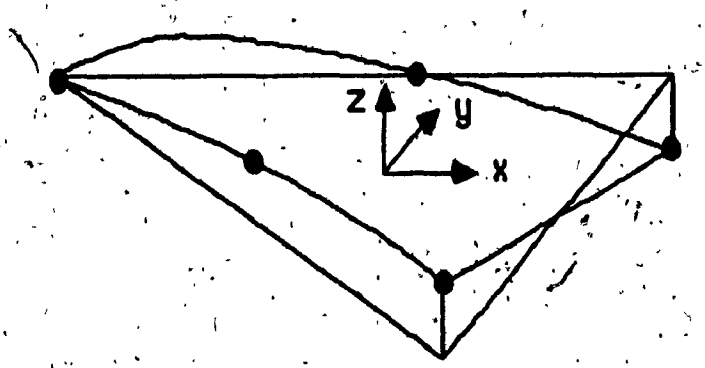

(b)

FIGURE 8.1: , ZERO ENERGY MODES FOR T9-2

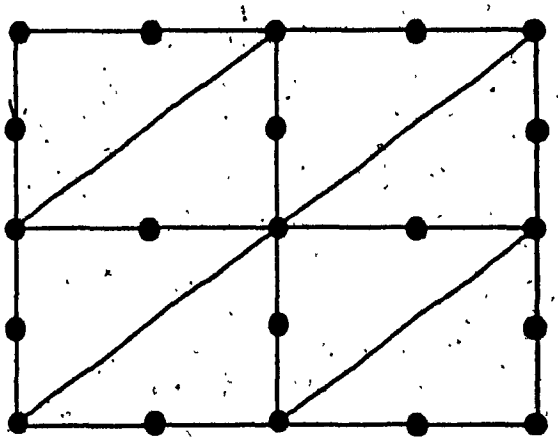

FIGURE 8.2: MESH ARRANGEMENT FOR T9-2

of clamped plate (Fig.(7.7)) are similar to those obtained by T17-3 and show little sensitivity to variations in the shear parameter. However, as mentioned in Chapter VII, the analytical solutions for lower shear parameters have been underestimated. The test results for moments at the mid-side of the clamped plate, in the shear parameter test, are comparable to those of other elements.

The results for T9-2, in the aspect ratio test, fall somewhere between the results for T17-3 and the other elements (Fig. (7.10) to (7.13)). For displacement at the center of the simply supported plate (Fig.(7.10)), the accuracy is not sensitive to changes in the aspect ratios of less than 2. For larger aspect ratios, the accuracy deteriorates rapidly. This is due to the existence of zero energy modes of Fig. (8.1). For the displacement at the center of the clamped plate (Fig. (7.11)), the results vary similarly to other elements for aspect ratios of less than 2 and after that the accuracy seems to improve. This behavior has not been observed in other elements.

The accuracy of results for M_{xx} and M_{yy} at the center of the simply supported plate (Fig.(7.12) and (7.13)) remains stable for aspect ratios less

than 2. For larger aspect ratios, the accuracy for M_{xx} improves whereas that of M_{yy} diminishes. The results for moments at the mid-side of clamped plate for different aspect ratios are comparable to those obtained using other elements.

In summary, this element seems to perform better than T17-3 but not as well as the other elements and in particular with respect to T9 and R11. The major shortcoming of this element, as with T17-3 , is its lack of stability for aspect ratios larger than 2. This lack of accuracy is caused by the existence of zero energy modes of Fig.(8.1) and (8.2) in this element.

CHAPTER IX

CONCLUSIONS

In this study, displacement and assumed stress hybrid finite elements capable of modelling three layer flat sandwich plates were considered.

In the formulation of the stiffness matrix for some of the displacement elements, a common rotation for the normals through the thickness is assumed. These elements are not recommended for the analysis of sandwich plates where severe discontinuities in the rotations of the normals may exist.

For other displacement elements, different rotations of the normals through the thickness are assumed. This is achieved by additional nodes and degrees of freedom through the thickness of the element. As a result, these elements are capable of modelling laminates with arbitrary material properties and thicknesses, thus can account for transverse shear deformations in each layer. Also, these elements are generally quite accurate. The accuracy and the wide range of applicability of these elements are at the expense of complex formulation and large number of

degrees of freedom. Furthermore, due to the existence of nodes through the thickness and non-geometric degrees of freedom, these elements are neither suitable for the analysis of three dimensional structures nor can they be integrated into general purpose structural analysis packages. Nevertheless, these elements are highly recommended for specialized problems involving flat plate configurations.

Among the displacement elements surveyed, Khatua and Cheung's elements [13,14] are most suitable for the analysis of sandwich plates. These elements are based on the assumptions of Chapter II and can be used to model orthotropic sandwich plates with thick faces. These elements have proven to be accurate in several numerical tests [13,14].

Formulation of the stiffness matrix for assumed stress hybrid elements is simpler than for displacement elements. Also, plate bending hybrid elements, in addition to being two dimensional in nature, require only geometric degrees of freedom, thus can be easily implemented in finite element packages. Furthermore, the range of capabilities of these elements can be easily modified by appropriately changing expressions for flexural and shear rigidities.

The disadvantages of hybrid elements are that their solutions are not

bounded and that the stiffness matrix for some elements may have zero energy modes.

The performance of several assumed stress hybrid elements capable of representing symmetric, three layer, flat sandwich plates with thin faces and isotropic materials were examined. In a set of numerical tests, the convergence characteristics of these elements were evaluated. Other numerical tests were performed in order to determine the influence of shear parameter and aspect ratio on the accuracy of these elements.

The adverse effect of unsuppressed zero energy modes on the accuracy of these elements is evident from the performance of T17-3 [5] and T9-2 elements. It was found that elements R11 [15] and T9 [7] perform well in all tests. Element T9 has one zero energy mode that does not occur in a mesh and element R11 has no zero energy modes. Therefore, the use of these elements is recommended for the above class of problems.

REFERENCES

1- Ahmad, S., Irons, B. M. and Zienkiewicz, O. C., "Analysis of Thick and Thin Shell Structures by Curved Finite Elements," IJNME, Vol. 2, 1970, pp. 419-451.

2- Albasiny, E. L. and Martin, D. W., "Bending and Membrane Equilibrium in Cooling Towers," J. Eng. Mech. Div. ASCE, EM3, 1967, pp. 1-17.

3- Allen, H. G., "Analysis and Design of Structural Sandwich Panels," Pergamon Press, London, 1969.

4- Azar, J. J., "Bending Theory of Multilayer Orthotropic Sandwich Plates," AIAA J., Vol. 6, 1968, pp. 2166-2169.

5- Barnard, A. J., "A Sandwich Plate Finite Element," The Mathematics of Finite Element and Applications, Proceedings of the Brunel University Conference of the Institute of Mathematics and Its Applications, held in April 1972, Academic Press, London, 1973, pp. 51-69.

6- Bartelds, G. and Ottens, H. H., "Finite Element Analysis of Sandwich Panels," Proceeding of IUTAM Symposium on High Speed Computing of Elastic Structures, University of Liege, Vol. 61, Tome 1,1971, pp. 357-382.

7- Cook, R. D., "Two Hybrid Elements for Analysis of Thick, Thin and Sandwich Plates," IJNME, Vol. 5, 1972, pp. 277-288.

8- Cook, R. D., "Some Elements for the Analysis of Plate Bending," J. of Eng. Mech. Div., ASCE, Vol. 98, No. EM6, 1972, pp. 1453-1470.

9- Cook, R. D. and Ladkany S. G., "Observations Regarding Assumed Stress Hybrid Plate Elements," IJNME, Vol. 8, 1974, pp. 513-519.

10- Cook, R. D., "Concepts and Applications of Finite Element Analysis," Second Edition, John Wiley and Sons Inc., 1981.

11- Ha, H. K., "Analysis of Three Dimensional Orthotropic Sandwich Plate Structures by Finite Element Method," Ph.D. Thesis, Faculty of Engineering, Concordia University, Montreal, 1972.

12- Henshell, R. D., "On Hybrid Finite Elements," Proceedings of Brunel University Conference of the Institute of Mathematics and Its Applications, 1972, pp. 299-311.

13- Khatua, T. P. and Cheung Y. K., "Triangular Element for Multilayer Sandwich Plates," J. of Eng. Mech. Div., ASCE, Vol. 98, EM5, 1972, pp. 1225-1238.

14- Khatua, T. P. and Cheung Y. K., "Bending and Vibration of Multilayer Sandwich Beams and Plates," IJNME, Vol. 6, No. 1, 1973, pp. 11-24.

15- Krishnan, G., "Analysis of Folded Sandwich Panel Roof System Using Assumed Stress Hybrid Elements," M.Eng. Thesis, Center for Building Studies, Concordia University, Montreal, 1984.

16- Lewis, W. C., "Supplement to: Deflection and Stresses in a Uniformly Loaded, Simply Supported Rectangular Sandwich Plate - Experimental Verification of Theory," FPL Report No. 1847-A, 1956.

17- Liaw, B. D. and Little, R. W., "Theory of Bending of Multilayer Sandwich Plates," AIAA J., Vol. 5, 1967, pp. 301-304.

18- Mau, S. T., Tong, P. and Pian, T. H. H., "Finite Element Solution for Laminated Thick Plates," J. of Composite Materials, Vol. 6, 1972, pp. 304-311.

19- Mawenya, A. S. and Davies, J. D., "Finite Element Bending Analysis of Multilayer Plates," IJNME, Vol. 8, 1974, pp. 215-225.

20- Monforton, G. R. and Schmidt, L. A. Jr., "Finite Element Analysis of Sandwich Plates and Cylindrical Shells with Laminated Faces," Proceedings of Second Conference on Matrix Methods in Structural Mechanics, Wright-Patterson Airforce Base, Ohio, AFFDL-TR-68-150, 1968, pp. 573-616.

21- Panda, S. C. and Natarajan, R., "Finite Element Analysis of Laminated Composite Plates," IJNME, Vol. 14, 1979, pp. 69-79.

22- Pagano, N. J., "Exact Solutions for Rectangular Bidirectional Composites and Sandwich Plates," J. of Composite Materials, Vol. 4, 1970, pp. 20-34.

23- Pagano, N. J., "Influence of Shear Coupling in Cylindrical Bending of Anisotropic Plates," J. of Composite Materials, Vol. 4, 1970, pp. 330-343.

24- Pagano, N. J. and Hatfield S. J., "Elastic Behavior of Multilayered Bidirectional Composites," AIAAJ., Vol. 10, 1972, pp. 931-933.

25- Pian, T. H. H., "Derivation of Element Stiffness Matrices by Assumed Stress Distributions," AIAAJ., Vol. 2, 1964, pp. 1333-1336.

26- Pian, T. H. H., "Element Stiffness Matrices for Boundary Compatibility and for Prescribed Boundary Stresses," Proceedings of the First Conference on Matrix Methods in Structural Mechanics, Wright-Patterson Airforce Base, Ohio, AFFDL-TR-66-80, 1966, pp. 457-477.

27- Pian, T. H. H. and Tong P., "Rationalization in Deriving Element Stiffness Matrix by Assumed Stress Approach," Proceedings of the Second Conference on Matrix Methods in Structural Mechanics, Wright-Patterson Airforce Base, Ohio, AFFDL-TR-68-150, 1968, pp. 441-469.

28- Pian, T. H. H. and Mau, S. T., "Some Recent Studies in Assumed Stress Hybrid Models," Advances in Computational Methods in Structural Mechanics and Design, University of Alabama Press, Alabama, 1972, pp. 87-106.

29- Plantema, F. J., "Sandwich Construction," John Wiley and Sons Inc., New York, 1966.

30- Pryor, C. W. Jr. and Barker, R. M., "A Finite Element Analysis Including Transverse Shear Effects For Application to Laminated Plates," AIAA J., Vol. 9, No. 5, 1971, pp. 912-917.

31- Reissner, E. and Stavsky, Y., "Bending and Stretching of Certain Types of AeolotrópicElastic Plates," J. of App. Mech., 1961, pp. 402-408.

32- Timoshenko, S., "Strength of Materials," Part II, Third Ed., Van Nostrand, New York, 1956, pp. 96-101.

33- Whitney, J. M., "The Effect of Transverse Shear Deformation on Bending of Laminated Plates," J. of Composite Materials, Vol. 3, 1969, pp. 534-547.

34- Zienkiewicz, O. C., "The Finite Element Method in Engineering Science," Second Ed., McGraw Hill, London, 1971.